Chapter 3

The Disturbance Field of a Single Particle in a Steady Flow

3.1 Introduction

In this chapter we consider the slow motion of a single particle in a viscous fluid and the nature of the disturbance produced by such motions on the ambient flow field. The study of the motion of a single particle in Stokes flow is an old subject and the earliest solutions have been known for more than a century. Nevertheless, a thorough understanding of the subject is a prerequisite for the more difficult task of determining hydrodynamic interactions between particles, the subject of the following chapter. Furthermore, in Part IV we shall use ideas developed in this and other chapters of Part II to derive analytic solutions to furnish concrete examples to back up the theorems — the theorems alone being somewhat abstract in nature. The presentation here is therefore cast in a form that is somewhat different from existing books on fluid dynamics, since our motivations and ultimate goals are different from these references.

The topics covered in the sections of this chapter range in complexity from the simple introduction of our notation to illustration of some subtle properties of Stokes flow. The multipole expansion for the disturbance field of a rigid particle, which was mentioned in the previous chapter, provides a familiar starting point for the discussion. We consider the form taken by rigid particles and viscous drops, as the two are different because of the slip velocity at the mobile interface. In Section 3.3, we examine those special cases and shapes for which the multipole expansion terminates or reduces to an analytical form. We derive some exact results for ellipsoids and show that the multipole expansion has a finite radius of convergence. For needle-like particles (Section 3.4) we discuss an approximate solution method based on line distribution of singularities, also known as *slender body theory*. A direct relation (Faxén laws) between the ambient flow and the coefficients of the multipole expansion is introduced in Section 3.5, thus completing the circle for a given disturbance problem.

3.2 The Far Field Expansion: Rigid Particles and Drops

From Chapter 2 we have the multipole expansion for the disturbance velocity field of a rigid particle immersed in an ambient field $\boldsymbol{v}^\infty$,

$$\boldsymbol{v} = \sum_{n=0}^{\infty} \frac{(-1)^n}{n!} \boldsymbol{L}^{(n)} \cdot \frac{\mathcal{G}(\boldsymbol{x})}{8\pi\mu} , \tag{3.1}$$

with

$$\boldsymbol{L}^{(n)} = \oint_{S_p} [(\boldsymbol{\sigma} \cdot \hat{\boldsymbol{n}}) \xi_{k_1} \dots \xi_{k_n}] \, dS \frac{\partial}{\partial x_{k_1}} \dots \frac{\partial}{\partial x_{k_n}} .$$

Equation 3.1 provides a completely general expression for $\boldsymbol{v}$. Each successive term introduces additional factors of a/r, where a is length scale based on the particle size; so the first few terms are sufficient to describe the effect of the particle far away from it. However, the computational procedure for the multipole coefficients (using the Faxén laws of Section 3.5) is quite tedious, so that in general the multipole expansion is not useful for velocity calculations, especially near the particle. The exception is for particles and flow fields possessing a high degree of symmetry, where the expansion terminates and further simplifications are possible. These so-called singularity solutions are discussed in the following section. We place the discussion of the Faxén relations after this because, for the general particle, the functional form of the Faxén relations is dictated by the singularity solution, as a consequence of the Lorentz reciprocal theorem. For the simplest geometry of all, the sphere, there are a number of other methods as well, but we defer to Chapter 4 a discussion of general solutions of the Stokes equations in spherical coordinates.

We now consider the extension of Equation 3.1 to the disturbance field of a viscous drop. There are subtle differences that can be traced to the slip velocity on the mobile interface and its effect on the integral representation. Of course, far away from the object the fundamental form of the solution cannot change; again we must have a multipole expansion in terms of Stokes monopoles, Stokes dipoles, Stokes quadrupoles, and so forth. Therefore, the differences between the disturbance field of a rigid particle and that produced by a viscous drop of the same dimension must manifest itself through the coefficients, *viz.*, the functional form taken by the force, stresslets, and other moments.

We repeat the steps of Section 2.4.3 for the integral representation for a disturbance field produced by a particle. For a stationary viscous drop, $\boldsymbol{v} \cdot \hat{\boldsymbol{n}} = 0$, but $\boldsymbol{v}$ itself is not zero – the interface is mobile. The integral representation is therefore (see Exercise 3.1)

$$\begin{aligned} \boldsymbol{v}(\boldsymbol{x}) - \boldsymbol{v}^\infty(\boldsymbol{x}) \;=\; & -\frac{1}{8\pi\mu} \oint_S (\boldsymbol{\sigma}(\boldsymbol{\xi}) \cdot \hat{\boldsymbol{n}}) \cdot \mathcal{G}(\boldsymbol{x} - \boldsymbol{\xi}) \, dS(\boldsymbol{\xi}) \\ & - \oint_S \boldsymbol{v}(\boldsymbol{\xi}) \cdot (\boldsymbol{\Sigma} \cdot \hat{\boldsymbol{n}}) \, dS(\boldsymbol{\xi}) \end{aligned}$$

and has both the single layer and double layer terms.

The Taylor expansion of the kernel of the single layer potential leads to the same functional forms encountered with the rigid particle. For the double layer term, we recall that

$$8\pi\mu\boldsymbol{\Sigma} = \mathcal{P}\boldsymbol{\delta} + \mu(\nabla\mathcal{G} + (\nabla\mathcal{G})^t) \ .$$

Since $\boldsymbol{v}\cdot\hat{\boldsymbol{n}} = 0$ at the interface, the fundamental pressure field makes no contribution to the velocity field generated by the double layer potential. In essence, the double layer potential is simply a distribution of symmetric Stokes dipoles over the interface, and the multipole expansion follows from the appropriate Taylor expansion. Consequently, the double layer potential contributes no force or torque, and to leading order in the expansion appears as a symmetric Stokes dipole located at the center of the drop.

We summarize the results for the viscous drop: The leading order terms are the Stokeslet and symmetric Stokes dipole, and the expressions for their coefficients (force and stresslet) are

$$\begin{aligned}
\boldsymbol{F} &= \oint_S (\boldsymbol{\sigma}\cdot\hat{\boldsymbol{n}})\, dS \\
\boldsymbol{S} &= \frac{1}{2}\oint_S [(\boldsymbol{\sigma}\cdot\hat{\boldsymbol{n}})\boldsymbol{\xi} + \boldsymbol{\xi}(\boldsymbol{\sigma}\cdot\hat{\boldsymbol{n}})]\, dS - \frac{1}{3}\oint_S (\boldsymbol{\sigma}\cdot\hat{\boldsymbol{n}})\cdot\boldsymbol{\xi}\, dS\ \boldsymbol{\delta} \\
&\quad - \mu\oint_S (\boldsymbol{v}\hat{\boldsymbol{n}} + \hat{\boldsymbol{n}}\boldsymbol{v})\, dS \ .
\end{aligned}$$

The identical result was obtained in Chapter 2 in the discussion on bulk stresses in a suspension. The "torque" on the drop is given formally by

$$\boldsymbol{T} = \oint_{S_p} \boldsymbol{\xi}\times(\boldsymbol{\sigma}\cdot\hat{\boldsymbol{n}})\, dS \ ,$$

but of course this is identically zero unless the drop fluid has an microstructure that endows it with an internal couple.

3.3 Singularity Solutions

For the general particle shape, the multipole expansion representation requires an infinite number of terms. Of course this is not a severe disadvantage in far field analyses, for in the far field the first few terms in the moment expansion capture the dominant behavior of the disturbance velocity field and at the same time provide information concerning the net hydrodynamic force, torque, *etc.* on the particle. In the near field, all terms in the expansion become comparable in magnitude, thus the multipole method becomes quite cumbersome unless some other simplifying factor enters into the picture. In this section, we shall show that for the sphere, the multipole expansion contains only a finite number of terms. For other simple shapes like the ellipsoid, a truncated expansion in just the lower order singularities is possible, provided that these singularities are distributed over a region. This collection of singularities and their region of

$$
\begin{aligned}
\mathcal{G}_{ij} &= \frac{1}{r}\delta_{ij} + \frac{1}{r^3}x_i x_j \ , \qquad r = |\boldsymbol{x}| \\
\mathcal{G}_{ij,k} &= \frac{1}{r^3}(-\delta_{ij}x_k + \delta_{jk}x_i + \delta_{ik}x_j) - \frac{3}{r^5}x_i x_j x_k \\
\nabla^2\mathcal{G}_{ij} &= \frac{2}{r^3}\delta_{ij} - \frac{6}{r^5}x_i x_j \\
\nabla^2\mathcal{G}_{ij,k} &= -\frac{6}{r^5}(\delta_{ij}x_k + \delta_{jk}x_i + \delta_{ik}x_j) + \frac{30}{r^7}x_i x_j x_k
\end{aligned}
$$

Table 3.1: The derivatives of the Oseen tensor and degenerate quadrupole.

distribution are collectively called the *image system*, and the resulting expressions are known as *singularity solutions*. A good starting point for a discussion of the singularity method for Stokes flow may be found in [20] and references therein, while [2] provides an excellent overview of the singularity method for a wide range of problems in mathematical physics.

Two final comments: The multipole expansion about the centroid of an ellipsoid and other particles for which singularity solutions are known can be expressed in closed form because the moments of the singularity distribution are easy to work out analytically. Also, we will restrict our attention in this section to the linear ambient flow, $\boldsymbol{U}^\infty + \boldsymbol{\Omega}^\infty \times \boldsymbol{x} + \boldsymbol{E}^\infty \cdot \boldsymbol{x}$.

3.3.1 Singularity System for Spheres

In electrostatics, we encounter the fact that the field of a point charge also provides the exact solution for a spherical perfect conductor. It is not surprising, then, that an analogous (but not identical) situation exists in Stokes flow. We shall consider the main flows of interest to microhydrodynamics (uniform stream, shear flows, extensional flows) and show that the multipole expansion does indeed contain a finite number of terms. At the beginning, we shall be content merely with demonstrations that the proposed solutions are correct (this is relatively straightforward). The more difficult task of explaining the solution philosophy and technique will be deferred until the end of the section.

Let us begin by examining the first few derivatives of the Oseen tensor $\mathcal{G}(\boldsymbol{x})$ and the degenerate quadrupole $\nabla^2\mathcal{G}(\boldsymbol{x})$. These expressions are used quite frequently and are listed in Table 3.1.

Consider the combination, $(1 + (a^2/6)\nabla^2)\mathcal{G}(\boldsymbol{x})$ evaluated on the surface of a sphere of radius a, $r = a$. From Table 3.1 we see that when $r = a$,

$$
(1 + \frac{a^2}{6}\nabla^2)\mathcal{G}(\boldsymbol{x}) = \frac{4}{3a}\boldsymbol{\delta} \ .
$$

From this, we immediately obtain the velocity field produced by a sphere trans-

lating with a steady velocity $\boldsymbol{U}$,

$$\boldsymbol{v}(\boldsymbol{x}) = 6\pi\mu a\boldsymbol{U}\cdot(1+\frac{a^2}{6}\nabla^2)\frac{\mathcal{G}(\boldsymbol{x})}{8\pi\mu}\ .$$

It is a straightforward exercise to show that this expression is identical to the standard result expressed in spherical coordinates given in elementary books on fluid mechanics (see also Chapter 4). We have obtained two results that merit further discussion. Firstly, whereas the conducting sphere of electrostatics can be represented by just the point charge or monopole field, *the translating sphere in Stokes flow requires a degenerate quadrupole* $a^2\boldsymbol{F}\nabla^2\delta(\boldsymbol{x})$, *in addition to a monopole of strength* $6\pi\mu a\boldsymbol{U}$. This apparently is due to the more complicated structure of the Stokes equation as compared to the Laplace equation. Secondly, *we have derived Stokes law,* $\boldsymbol{F} = -6\pi\mu a\boldsymbol{U}$ *for the drag on a sphere undergoing steady translation, without explicit computation of surface tractions.* This illustrates the point that was raised earlier that solutions expressed as a multipole expansion yield quantities of interest, such as the hydrodynamic force, in a straightforward fashion.

Example 3.1 The Rotating Sphere.
From Table 3.1 we see that when $r = a$, the antisymmetric part of the Stokes dipole satisfies

$$\frac{1}{2}(\mathcal{G}_{ij,k} - \mathcal{G}_{ik,j}) = \frac{1}{a^3}(\delta_{ik}x_j - \delta_{ij}x_k)\ .$$

The velocity field of a rotating sphere in the ambient flow $\boldsymbol{\Omega}^\infty \times \boldsymbol{x}$ may be written as

$$\begin{aligned}\boldsymbol{v}(\boldsymbol{x}) - \boldsymbol{\Omega}^\infty\times\boldsymbol{x} &= -4\pi\mu a^3[\boldsymbol{\epsilon}\cdot(\boldsymbol{\Omega}^\infty-\boldsymbol{\omega})\cdot\nabla]\cdot\frac{\mathcal{G}(\boldsymbol{x})}{8\pi\mu}\\ &= a^3(\boldsymbol{\Omega}^\infty-\boldsymbol{\omega})\times\nabla\frac{1}{r} = (\boldsymbol{\omega}-\boldsymbol{\Omega}^\infty)\times\boldsymbol{x}\frac{a^3}{r^3}\ ,\end{aligned}$$

in agreement with Lamb's general solution. In conclusion, the rotating sphere may be represented with just a *rotlet* and $\boldsymbol{T} = 8\pi\mu a^3(\boldsymbol{\Omega}^\infty - \boldsymbol{\omega})$ is the torque exerted by the fluid on the sphere.◇

Example 3.2 The Sphere in a Rate-of-Strain Field.
From Table 3.1 we see that when $r = a$,

$$(1+\frac{a^2}{10}\nabla^2)(\mathcal{G}_{ij,k} + \mathcal{G}_{ik,j}) = -\frac{6}{5a^3}(\delta_{ik}x_j + \delta_{ij}x_k - \frac{2}{3}\delta_{jk}x_i)\ .$$

From this, we get immediately the velocity field produced by a fixed sphere in the straining field $\boldsymbol{E}^\infty\cdot\boldsymbol{x}$,

$$\boldsymbol{v}(\boldsymbol{x}) - \boldsymbol{E}^\infty\cdot\boldsymbol{x} = \frac{20}{3}\pi\mu a^3(\boldsymbol{E}^\infty\cdot\nabla)\cdot(1+\frac{a^2}{10}\nabla^2)\frac{\mathcal{G}(\boldsymbol{x})}{8\pi\mu}\ .$$

The fixed sphere in a straining field may be represented by a stresslet of strength $(20/3)\pi\mu a^3\boldsymbol{E}^\infty$ and a degenerate octupole $a^2(\boldsymbol{S}\cdot\nabla)\nabla^2\delta(\boldsymbol{x})$.◇

This procedure is readily generalized to higher order fields. The reader is encouraged to examine the linear combination

$$\mathcal{G}_{ij,k_1\ldots k_n} + \frac{a^2}{4n+6}\nabla^2\mathcal{G}_{ij,k_1\ldots k_n}$$

to investigate its suitability as a solution for a sphere in an n-th order ambient field.

3.3.2 The Spherical Drop and Interior Flows

For interior flows the *Stokeson* is the analog of the Stokeslet [20], since it too is linear with respect to a constant vector $\boldsymbol{U}$. The velocity field of the Stokeson may be written as

$$\begin{aligned} v_i = \mathcal{H}_{ij}U_j &= (2r^2\delta_{ij} - x_ix_j)U_j \\ p &= 10\mu\boldsymbol{x}\cdot\boldsymbol{U}\ . \end{aligned}$$

It should come as no surprise that the Stokeson enters into the solution for the translating spherical drop, since the interior solution must be linear with respect to $\boldsymbol{U}$, and $\boldsymbol{U}\cdot\mathcal{H}$ meets this criterion. Indeed, the solution for the translating drop can be constructed using a Stokeslet and a degenerate quadrupole outside and a Stokeson and a uniform field $\boldsymbol{U}$ inside the drop. The velocity fields inside and outside the drop are written as

$$\begin{aligned} \boldsymbol{v}^{(i)} &= D_0\hat{\boldsymbol{U}} + D_2a^{-2}\boldsymbol{U}\cdot\mathcal{H}(\boldsymbol{x}) \\ \boldsymbol{v}^{(o)} &= \frac{3a}{4}\boldsymbol{U}\cdot(C_0 + C_2a^2\nabla^2)\mathcal{G}(\boldsymbol{x}) \end{aligned}$$

to satisfy the boundary condition for large r and at $r = 0$. The boundary conditions at the drop interface provide the equations to determine the four unknown constants.

At $r = a$, the boundary conditions on the radial and tangential velocities and the tangential component of the surface traction $\boldsymbol{\sigma}\cdot\boldsymbol{n}$ are

1. $\hat{\boldsymbol{n}}\cdot\boldsymbol{v}^{(o)} = \hat{\boldsymbol{n}}\cdot\boldsymbol{U}$
2. $\hat{\boldsymbol{n}}\cdot\boldsymbol{v}^{(i)} = \hat{\boldsymbol{n}}\cdot\boldsymbol{U}$
3. $\boldsymbol{v}^{(o)} - \hat{\boldsymbol{n}}\hat{\boldsymbol{n}}\cdot\boldsymbol{v}^{(o)} = \boldsymbol{v}^{(i)} - \hat{\boldsymbol{n}}\hat{\boldsymbol{n}}\cdot\boldsymbol{v}^{(i)}$
4. $(\boldsymbol{e}^{(o)}\cdot\hat{\boldsymbol{n}})\cdot(\boldsymbol{\delta} - \hat{\boldsymbol{n}}\hat{\boldsymbol{n}}) = \lambda(\boldsymbol{e}^{(i)}\cdot\hat{\boldsymbol{n}})\cdot(\boldsymbol{\delta} - \hat{\boldsymbol{n}}\hat{\boldsymbol{n}})$

where $\lambda = \mu^{(i)}/\mu^{(o)}$, the ratio of the drop and solvent viscosities. Here, C_0 and C_2, are the quantities of greatest interest, and the final results are

$$\begin{aligned} C_0 &= \frac{2+3\lambda}{3(1+\lambda)} \\ C_2 &= \frac{\lambda}{6(1+\lambda)}\ . \end{aligned}$$

For large λ, we obtain the singularity solution for the rigid sphere, while for $\lambda = 0$ (bubble), the degenerate quadrupole vanishes. The Stokeslet alone provides the exact solution for a translating bubble.

Other interior solutions appear in the context of a viscous drop in the n-th order field. The gradient of the Stokeson is a third-order tensor that is linear in r (because the Stokeson is quadratic in r). The symmetric and antisymmetric derivatives are known as the *roton* and *stresson* [20] in analogy with the rotlet and stresslet. These are in fact rarely used as such, since the roton and stresson simply correspond to a rigid-body rotation and a constant rate-of-strain field. They (*i.e.*, the rotational and rate-of-strain fields), together with a field that is cubic in r. are used in the construction of the interior flow field for a spherical drop in the linear field $\boldsymbol{\Omega} \times \boldsymbol{x} + \boldsymbol{E} \cdot \boldsymbol{x}$. The cubic field is in fact the less obvious portion of the solution, but it can be obtained either from Lamb's general solution or by the appropriate linear combination of $\boldsymbol{E} : \boldsymbol{xxx}$ and $\boldsymbol{E} \cdot \boldsymbol{x}r^2$.

3.3.3 Singularity System for Ellipsoids

The ellipsoid is encountered frequently in mathematical physics because it is a relatively simple nonaxisymmetric shape. Our analysis for the ellipsoid also provides a unified approach to a number of hydrodynamic problems, for the general ellipsoid contains a broad class of shapes ranging from disks to needles. Admittedly, a discussion on spheroids (ellipsoids of revolution) would introduce a smaller jump and would provide a more gradual rise in the demands placed on the reader. However, our major goal here is to show that a surprisingly simple and general approach to the flow past an ellipsoid exists.

Consider a general triaxial ellipsoid with coordinates chosen so that the surface of the ellipsoid is given by the expression

$$\frac{x^2}{a^2} + \frac{y^2}{b^2} + \frac{z^2}{c^2} = 1 \ , \tag{3.2}$$

with $a \geq b \geq c$. Initially, we expect a great jump in complexity going from the singularity solution for the sphere to that for the general ellipsoid. The three fundamental problems — *translation*, *rotation*, and *linear ambient field* — are solved in the papers of Oberbeck [63], Edwardes [26], and Jeffery [46]. These original solutions in ellipsoidal coordinates, collected in the first part of Table 3.2, are certainly intricate and apparently defy further analysis. (Readers interested in further study of ellipsoidal harmonics are directed to Hobson's treatise [42].) Our goal here is to formulate a solution method based on the multipole expansion and certain theorems from potential theory that provides a uniform framework for derivation of these as well as other flow fields involving the ellipsoid. We shall first present the final result and then provide the derivation. Various degenerate cases, such as the ellipsoid of revolution, are of great interest and take up the remainder of the discussion.

The solutions in Table 3.2 are special cases of the solutions for the n-th order ambient velocity field,

$$v_i^\infty = H_{ik_1k_2\ldots k_n} x_{k_1} x_{k_2} \ldots x_{k_n} \ . \tag{3.3}$$

Bilevel indices are used to avoid the introduction of n different subscript variables.

The solution to this problem will be presented, first in the singularity form, and then in terms of ellipsoidal harmonics, which includes the classical solutions as special cases. The transformation from the singularity solution to the multipole expansion is shown at the end of this subsection.

The disturbance velocity for an $(n-1)$-th order ambient field is explicitly

$$v_i = \sum_{m=0}^{[(n-1)/2]} L_{(n-2m)\,j} \int_E f_{(n-2m)}(\boldsymbol{x}')\{1 + \frac{c^2 q^2 \nabla^2}{4(n-2m)-2}\}\frac{\mathcal{G}_{ij}(\boldsymbol{x}-\boldsymbol{x}')}{8\pi\mu} dA(\boldsymbol{x}') \,, \tag{3.4}$$

with

$$\begin{aligned} f_{(n)}(\boldsymbol{x}) &= \frac{(2n-1)q^{(2n-3)}}{2\pi a_E b_E} \,, \qquad q(\boldsymbol{x}) = \sqrt{1 - x^2/a_E^2 - y^2/b_E^2} \,, \\ a_E &= \sqrt{a^2 - c^2} \,, \quad b_E = \sqrt{b^2 - c^2} \,, \\ L_{(n)j} &= \frac{(-1)^n}{(n-1)!} P_{jk_1k_2\ldots k_{n-1}} \frac{\partial}{\partial x_{k_1}} \frac{\partial}{\partial x_{k_2}} \cdots \frac{\partial}{\partial x_{k_{n-1}}} \,. \end{aligned}$$

Thus, an n-th order ambient field with n even (odd), induces a distribution of all even (odd) multipole moments up to and including the n-th moment. The pressure, p, is obtained by an analogous distribution of the fundamental pressure field. The constant tensors $\boldsymbol{P}$ give the strengths of the distributed multipole moments. The first two, P_j and P_{jk}, are the force and stress dipole. The precise relation between the $\boldsymbol{P}$'s and the multipole moments taken about the particle center is examined later. For now, we simply note that the solution method includes a procedure for their evaluation. Finally, the focal ellipse $E(\boldsymbol{x}')$,

$$\frac{x'^2}{a_E^2} + \frac{y'^2}{b_E^2} \le 1 \,, \quad z = 0 \,, \tag{3.5}$$

is the degenerate elliptical disk in the family of ellipsoids that are confocal to the particle ellipsoid. Their role as the image system in potential flow is discussed in Miloh [61].

We will also derive an alternate form of Equation 3.4 expressed in terms of the ellipsoidal harmonic G_n of Table 3.2. This alternate solution is

$$\begin{aligned} v_i = \sum_{m=0}^{[(n-1)/2]} & \frac{(-1)^{n-2m-1}(n-2m)(2n-4m)!}{2^{2n-4m}\,(n-2m)!\,(n-2m)!} \frac{L_{(n-2m)\,j}}{8\pi\mu} \\ & \times \{(\delta_{ij} - x_j\frac{\partial}{\partial x_i})G_{n-2m-1} + \frac{a_j^2}{2(n-2m)}\frac{\partial^2}{\partial x_i \partial x_j} G_{n-2m}\} \,. \end{aligned} \tag{3.6}$$

There is a summation over j and the notation a_j for $j = 1, 2, 3$ has been introduced for a, b, c. For $n = 1$ and 2, this form is precisely the appropriate classical solution in Table 3.2.

1. Solution in Ellipsoidal Coordinates [26, 46, 63]

$$v_i - U_i^\infty = -\frac{F_j}{16\pi\mu}\left[\delta_{ij}G_0 - x_j\frac{\partial G_0}{\partial x_i} + \frac{a_j^2}{2}\frac{\partial^2 G_1}{\partial x_i \partial x_j}\right]$$

$$v_i - (\boldsymbol{\Omega}^\infty \times \boldsymbol{x} + \boldsymbol{E}^\infty \cdot \boldsymbol{x})_i = \frac{-3}{32\pi\mu}(\boldsymbol{S}\cdot\nabla + \frac{1}{2}\boldsymbol{T}\times\nabla)_j\left[\delta_{ij}G_1 - x_j\frac{\partial G_1}{\partial x_i} + \frac{a_j^2}{4}\frac{\partial^2 G_2}{\partial x_i \partial x_j}\right]$$

$$G_n = \int_\lambda^\infty \left(\frac{x^2}{a^2+t} + \frac{y^2}{b^2+t} + \frac{z^2}{c^2+t} - 1\right)^n \frac{dt}{\Delta(t)} ,$$

with $\Delta(t) = \sqrt{(a^2+t)(b^2+t)(c^2+t)}$ and the ellipsoidal coordinate $\lambda(x,y,z)$ defined as the postive root of

$$\frac{x^2}{a^2+t} + \frac{y^2}{b^2+t} + \frac{z^2}{c^2+t} = 1 .$$

The relation between $\boldsymbol{F}$, $\boldsymbol{T}$, and $\boldsymbol{S}$ and the $\boldsymbol{U}^\infty - \boldsymbol{U}$, $\boldsymbol{\Omega}^\infty - \boldsymbol{\omega}$, and $\boldsymbol{E}^\infty$ are given in Table 3.3.

2. Singularity Solutions

$$\boldsymbol{v} - \boldsymbol{U}^\infty = -\boldsymbol{F}\cdot\int_E f_{(1)}(\boldsymbol{x}')\{1 + \frac{c^2q^2\nabla^2}{2}\}\frac{\mathcal{G}(\boldsymbol{x}-\boldsymbol{x}')}{8\pi\mu}dA(\boldsymbol{x}')$$

$$\boldsymbol{v} - \boldsymbol{\Omega}^\infty\times\boldsymbol{x} - \boldsymbol{E}^\infty\cdot\boldsymbol{x} = (\boldsymbol{S}\cdot\nabla + \frac{1}{2}\boldsymbol{T}\times\nabla)\cdot\int_E f_{(2)}(\boldsymbol{x}')\{1+\frac{c^2q^2\nabla^2}{6}\}\frac{\mathcal{G}(\boldsymbol{x}-\boldsymbol{x}')}{8\pi\mu}dA(\boldsymbol{x}')$$

$$f_{(n)}(\boldsymbol{x}) = \frac{(2n-1)q^{2n-3}}{2\pi a_E b_E} , \qquad q(\boldsymbol{x}) = \sqrt{1 - x^2/a_E^2 - y^2/b_E^2} ,$$

$$a_E = \sqrt{a^2 - c^2} , \quad b_E = \sqrt{b^2 - c^2} .$$

3. Multipole Expansions

$$\boldsymbol{v} - \boldsymbol{U}_i^\infty = -\boldsymbol{F}\cdot\left(\frac{\sinh D}{D}\right)\frac{\mathcal{G}(\boldsymbol{x})}{8\pi\mu}$$

$$\boldsymbol{v} - \boldsymbol{\Omega}^\infty\times\boldsymbol{x} - \boldsymbol{E}^\infty\cdot\boldsymbol{x} = (\boldsymbol{S}\cdot\nabla + \frac{1}{2}\boldsymbol{T}\times\nabla)\cdot\left(\frac{3}{D}\frac{\partial}{\partial D}\right)\left(\frac{\sinh D}{D}\right)\frac{\mathcal{G}(\boldsymbol{x})}{8\pi\mu}$$

$$D^2 = a^2\frac{\partial^2}{\partial x^2} + b^2\frac{\partial^2}{\partial y^2} + c^2\frac{\partial^2}{\partial z^2} .$$

Table 3.2: The solutions for an ellipsoid in rigid-body motion $\boldsymbol{U} + \boldsymbol{\omega}\times\boldsymbol{x}$ in the ambient fields $\boldsymbol{U}^\infty$ and $\boldsymbol{\Omega}^\infty\times\boldsymbol{x} + \boldsymbol{E}^\infty\cdot\boldsymbol{x}$.

$$
\begin{aligned}
F_x &= \frac{16\pi\mu abc}{\chi_0 + \alpha_0 a^2}(U_x^\infty - U_x) \\
T_x &= \frac{16\pi\mu abc}{3(b^2\beta_0 + c^2\gamma_0)}\left[(b^2+c^2)(\Omega_x^\infty - \omega_x) + (b^2-c^2)E_{yz}^\infty\right] \\
S_{xx} &= \frac{16\pi\mu abc}{9(\beta_0''\gamma_0''\gamma_0''\alpha_0'' + \alpha_0''\beta_0'')}\left[2\alpha_0'' E_{xx}^\infty - \beta_0'' E_{yy}^\infty - \gamma_0'' E_{zz}^\infty\right] \\
S_{xy} = S_{yx} &= \frac{8\pi\mu abc}{3(a^2\alpha_0 + b^2\beta_0)}\left[(a^2-b^2)(\Omega_z^\infty - \omega_z) + \frac{(\alpha_0+\beta_0)}{\gamma_0'}E_{xy}^\infty\right]
\end{aligned}
$$

The χ_0, α_0, β_0, γ_0, α_0', β_0', γ_0', α_0'', β_0'', and γ_0'' are constant (elliptic integrals) that are obtained by evaluating the ellipsoidal harmonics at the surface $\lambda = 0$:

$$
\chi_0 = abcG_0(0) \ , \qquad \alpha_0 = abc\int_0^\infty \frac{dt}{(a^2+t)\Delta(t)} \ .
$$

The constants β_0 and γ_0 are obtained by successive cycling of the dependence on a, b, and c. The primed and double-primed constants are defined by

$$
\alpha' = \frac{\gamma - \beta}{b^2 - c^2} \ , \qquad \alpha'' = \frac{b^2\beta - c^2\gamma}{b^2 - c^2} \ ,
$$

with the rest defined by cycling a, b, and c and α, β, and γ. The notation shows the common pattern in these solutions; consequently our notation differs from the original works. There is a summation over j in the velocity expressions and the notation a_j for $j = 1, 2, 3$ is used for a, b, c.

Table 3.3: The *resistance relations* between the force, torque, and stresslet and the ambient flow in the solutions of Oberbeck, Edwardes, and Jeffery.

The harmonics $\chi(\lambda)$ and Ω (the Dirichlet potential) that appear in the solution of Oberbeck (see also [35]) are proportional to G_0 and G_1:

$$\chi = abcG_0 \ , \qquad \Omega = \pi abcG_1 \ .$$

We now show that the two solutions, Equations 3.4 and 3.6, are equivalent and that they satisfy the appropriate boundary conditions.

We first establish the singularity representations for the ellipsoidal harmonic G_n. We define

$$H_n = \int_E \frac{q^{2n-1}}{2\pi a_E b_E} \frac{dA(\boldsymbol{x}')}{|\boldsymbol{x} - \boldsymbol{x}'|} \tag{3.7}$$

and show that

$$H_n = \frac{(-1)^n \ (2n)!}{2^{2n+1} \ n! \ n!} \ G_n \ . \tag{3.8}$$

This also establishes that G_n is a harmonic.

For $n = 0$, Equation 3.8 is equivalent to the singularity representation for $\chi(\lambda)$ and follows from an application of Gauss' law to the potential field of an elliptic disk at constant potential [61]. Therefore, we assume that Equation 3.8 holds for n and show that this, in turn, implies that it holds for $n + 1$. To do this, we first establish the following relations:

$$G_{n+1}(\boldsymbol{x}; 1) = -2(n+1) \int_0^1 u^{2n+2} G_n(\boldsymbol{x}; u) \, du \ , \tag{3.9}$$

$$H_{n+1}(\boldsymbol{x}; 1) = (2n+1) \int_0^1 u^{2n+2} H_n(\boldsymbol{x}; u) \, du \ . \tag{3.10}$$

The parameter u in $G_n(\boldsymbol{x}; u)$ and $H_n(\boldsymbol{x}; u)$ denotes that the particle size has been scaled with u, *i.e.*, a, b, and c are replaced by ua, ub, and uc. The original ellipsoid corresponds to $u = 1$. We shall refer to the integral operations on the RHS of the preceding equations as *geometric scaling transformations.*

These relations are verified by direct integration. For example, Equation 3.9 is obtained in the following manner: Start with the definition of $G_n(\boldsymbol{x}, u)$ and integrate both sides with respect to u, changing variables from t to $\tau = u^2 t$. This yields

$$\int_0^1 u^{2n+2} G_n(\boldsymbol{x}; u) du = \int_0^1 u \int_{v(u)}^{\infty} \left(\frac{x^2}{a^2+\tau} + \frac{y^2}{b^2+\tau} + \frac{z^2}{c^2+\tau} - u^2\right)^n \frac{d\tau}{\Delta(\tau)} du,$$

where $v(u) = \lambda/u^2$. Now change the order of integration so that the double integral is performed over the region $\lambda \leq \tau \leq \infty$ and $v^{-1}(\tau) \leq u \leq 1$, with

$$v^{-1}(\tau) = \left[\frac{x^2}{a^2+\tau} + \frac{y^2}{b^2+\tau} + \frac{z^2}{c^2+\tau}\right]^{1/2} .$$

Consequently,

$$\int_0^1 u^{2n+2} G_n(\boldsymbol{x}; u) du = \int_\lambda^\infty \left[\int_{v^{-1}(\tau)}^1 (v^{-1}(\tau)^2 - u^2)^n u \, du\right] \frac{d\tau}{\Delta(\tau)} \ ,$$

and the integration with respect to u leads to Equation 3.9. Analogous steps may be used to derive Equation 3.10.

The induction to the case $n+1$ from the case n is accomplished by u-integration of both sides of Equation 3.8 with weights chosen as in Equations 3.9 and 3.10. The result is

$$H_{n+1} = \frac{(-1)^{n+1}\,(2n+2)!}{2^{2n+3}\,(n+1)!\,(n+1)!} G_{n+1}\ ,$$

which completes the proof.

The singularity solution may be rearranged into the harmonic representation by using the following identities involving the Oseen tensor:

$$\mathcal{G}_{ij}(\boldsymbol{x}-\boldsymbol{x}') = \delta_{ij}\frac{1}{|\boldsymbol{x}-\boldsymbol{x}'|} - (x-x')_j\frac{\partial}{\partial x_i}\left[\frac{1}{|\boldsymbol{x}-\boldsymbol{x}'|}\right] \tag{3.11}$$

$$\nabla^2\mathcal{G}(\boldsymbol{x}-\boldsymbol{x}') = -2\nabla\nabla\frac{1}{|\boldsymbol{x}-\boldsymbol{x}'|} \tag{3.12}$$

$$\int_E x'_j q^n \frac{dA(\boldsymbol{x}')}{|\boldsymbol{x}-\boldsymbol{x}'|} = -\frac{(a_j^2-c^2)}{(n+2)}\frac{\partial}{\partial x_j}\int_E \frac{q^{n+2}dA(\boldsymbol{x}')}{|\boldsymbol{x}-\boldsymbol{x}'|}\ . \tag{3.13}$$

The last equation follows from an integration by parts.

From Equation 3.6 it is clear that the evaluation of $\boldsymbol{v}$ on the ellipsoid surface requires knowledge of the values taken by $\partial^n G_n$ and $\partial^{n+1} G_n$ on the surface. (When the tensorial subscripts are obvious, the notation will be simplified by using ∂^n as the n-th derivative.) These derivatives are obtained by successive application of the Leibniz rule, with the additional simplification that the integrand of G_n evaluated at λ vanishes (by definition of λ). Thus

$$\partial G_n = 2nx_{k_1}\int_\lambda^\infty \frac{F^{n-1}}{(a_{k_1}^2+t)}\frac{dt}{\Delta(t)}$$

$$\partial^2 G_n = 4n(n-1)x_{k_1}x_{k_2}\int_\lambda^\infty \frac{F^{n-2}}{(a_{k_1}^2+t)(a_{k_2}^2+t)}\frac{dt}{\Delta(t)} + 2n\delta_{k_1k_2}\int_\lambda^\infty \frac{F^{n-1}}{(a_{k_1}^2+t)}\frac{dt}{\Delta(t)}\ ,$$

with

$$F = \frac{x^2}{a^2+t} + \frac{y^2}{b^2+t} + \frac{z^2}{c^2+t} - 1\ ,$$

until

$$\partial^n G_n = \sum_{m=0}^{[n/2]} 2^{n-m}\frac{n!}{m!}\{\delta_{k_1k_2}\ldots\delta_{k_{2m-1}k_{2m}}x_{k_{2m+1}}\ldots x_{k_n} \times \int_\lambda^\infty \frac{F^m}{[\Pi_{\alpha=1}^n(a_{k_\alpha}^2+t)]}\frac{dt}{\Delta(t)} + \cdots\ (sym)\ \}$$

($\alpha \neq k_2, k_4, \ldots, k_{2m}$ for term shown). The "(sym)" in the preceding expression denotes that at each m we must take all permutations of the indices k_i and that only one representative term has been shown explicitly.

At the summation index m, there are $n!/(2^m m!(n-2m)!)$ terms corresponding to all possible permutations of $\{k_1 \ldots k_n\}$ in the representative term. The key idea is that on the ellipsoid surface, $\lambda = 0$, the definite integrals become numerical constants that depend only on the shape of the ellipsoid. *Thus $\partial^n G_n$ reduces to a polynomial in $\boldsymbol{x}$ of degree n.*

The velocity expression also involves terms of the form $\partial^{n+1} G_n$, which we now proceed to evaluate at the ellipsoid surface:

$$\begin{aligned} \partial^{n+1} G_n &= -2^n n! x_{k_1} \ldots x_{k_n} \frac{1}{[\Pi_{\alpha=1}^n a_{k_\alpha}^2]\Delta(\lambda)} \frac{\partial \lambda}{\partial x_{k_{n+1}}} \\ &\quad + \text{ polynomial of degree } n-1. \end{aligned} \tag{3.14}$$

At the surface $\lambda = 0$,

$$\frac{\partial \lambda}{\partial x_k} = \frac{2x_k}{a_k^2} \left[\sum_{l=1}^{3} \frac{x_l^2}{a_l^4} \right]^{-1} .$$

Thus the leading order term in Equation 3.14 is not of the form specified in the boundary condition for the $(n-1)$-th order ambient field. In other words, the proposed velocity representation will have the proper behavior at the ellipsoid surface if and only if this $(n+1)$-th order field is canceled. There are only two such terms in the velocity representation of Equation 3.6. They occur in the second and third terms when $m = 0$, *i.e.*,

$$-x_j \partial^n G_n = 2^n (n-1)! x_i x_j x_{k_1} \ldots x_{k_{n-1}} ([\Pi_{\alpha=1}^n a_{k_\alpha}^2]\Delta(0)[\sum_{l=1}^{3} \frac{x_l^2}{a_l^4}])^{-1} + \cdots$$

$$\frac{a_j^2}{2n} \partial^{n+1} G_n = -2^n (n-1)! x_i x_j x_{k_1} \ldots x_{k_{n-1}} a_j^2 ([\Pi_{\alpha=1}^{n+1} a_{k_\alpha}^2]\Delta(0)[\sum_{l=1}^{3} \frac{x_l^2}{a_l^4}])^{-1} + \cdots .$$

In the second equation, a_j^2 may be eliminated so the two unwanted terms cancel each other. Thus, the velocity field evaluated at the surface of the ellipsoid is in fact a polynomial in $\boldsymbol{x}$ of degree $(n-1)$. The lower order fields (with the order successively decreasing by two) may be eliminated by repeated use of the preceding argument, *i.e.*, by mathematical induction. Thus the velocity may be expressed as in Equations 3.4 or 3.6 as claimed.

The last step in the solution procedure requires the determination of the $\boldsymbol{P}$ in terms of $\boldsymbol{H}$, the known gradients of the ambient field. This final step is accomplished by inverting the set of linear equations for the unknown tensorial coefficients. The symmetry in the ellipsoid geometry decouples the system so that the lower order cases $n = 1, 2, 3$ may be inverted analytically.

The singularity and ellipsoidal-harmonic forms of the velocity field are needed when exact computations of the velocity are required. We now derive the form most useful for far field analyses, the *multipole expansion*. The central identity in this discussion is the following:

$$\begin{aligned} \int_E f_{(1)}(\boldsymbol{x}') \{1 + \frac{c^2 q^2 \nabla^2}{2}\} \mathcal{G}(\boldsymbol{x} - \boldsymbol{x}')\, dA(\boldsymbol{x}') &= \left(\frac{\sinh D}{D} \right) \mathcal{G}(\boldsymbol{x}) \\ &= \left(1 + \frac{D^2}{3!} + \frac{D^4}{5!} + \cdots \right) \mathcal{G}(\boldsymbol{x}) , \end{aligned} \tag{3.15}$$

where, as shown, the operator on the right-hand side is defined formally by the power series in D^2, with $D^2 = a^2\partial^2/\partial x^2 + b^2\partial^2/\partial y^2 + c^2\partial^2/\partial z^2$. We note that D^2 can also be written as $D^2 = \tilde{D}^2 + c^2\nabla^2$ with $\tilde{D}^2 = a_E^2\partial^2/\partial x^2 + b_E^2\partial^2/\partial y^2$.

Since the operands are *biharmonic* functions, the higher powers of D^2 may be expanded as $D^{2k} = \tilde{D}^{2k} + c^2 k\tilde{D}^{2k-2}\nabla^2$, and, therefore, the symbolic operator on the RHS of Equation 3.15 becomes

$$\begin{aligned}\frac{\sinh D}{D} &= \frac{\sinh \tilde{D}}{\tilde{D}} + c^2 \sum_{k=1}^{\infty} \frac{k\tilde{D}^{2k-2}}{(2k+1)!}\nabla^2 \\ &= \frac{\sinh \tilde{D}}{\tilde{D}} + \frac{c^2}{2}\left(\frac{1}{\tilde{D}}\frac{\partial}{\partial \tilde{D}}\right)\left(\frac{\sinh \tilde{D}}{\tilde{D}}\right)\nabla^2 .\end{aligned}$$

Equation 3.15 now follows by matching the terms in $\mathcal{G}$ and $\nabla^2\mathcal{G}$. We show that

$$\begin{aligned}\int_E f_{(1)}(\boldsymbol{x}')\mathcal{G}(\boldsymbol{x}-\boldsymbol{x}')dA(\boldsymbol{x}') &= \left(\frac{\sinh \tilde{D}}{\tilde{D}}\right)\mathcal{G}(\boldsymbol{x}) \\ \int_E f_{(1)}(\boldsymbol{x}')q^2\nabla^2\mathcal{G}(\boldsymbol{x}-\boldsymbol{x}')dA(\boldsymbol{x}') &= \left(\frac{1}{\tilde{D}}\frac{\partial}{\partial \tilde{D}}\right)\left(\frac{\sinh \tilde{D}}{\tilde{D}}\right)\nabla^2\mathcal{G}(\boldsymbol{x}) .\end{aligned}$$

These two equations follow from identities concerning the surface tractions on an ellipsoid established by Brenner [12].[1]

For the singularity solution of arbitrary order we must establish the identity,

$$\begin{aligned}&\int_E f_{(n)}(\boldsymbol{x}')\{1 + \frac{c^2q^2\nabla^2}{4n-2}\}(\nabla)^{n-1}\mathcal{G}(\boldsymbol{x}-\boldsymbol{x}')dA(\boldsymbol{x}') \\ &= \frac{(2n)!}{2^n n!}\{\left(\frac{1}{D}\frac{\partial}{\partial D}\right)^{n-1}\left(\frac{\sinh D}{D}\right)\}(\nabla)^{n-1}\mathcal{G}(\boldsymbol{x}) \\ &= \frac{(2n)!}{n!}\sum_{k=1}^{\infty}\frac{(k+n-1)!\ D^{2k-2}}{(k-1)!\ (2k+2n-2)!}(\nabla)^{n-1}\mathcal{G}(\boldsymbol{x}) . \qquad (3.16)\end{aligned}$$

The left-hand side of Equation 3.16 can be generated by successive applications of the geometric similarity transformation. If we define

$$\boldsymbol{J}_n(\boldsymbol{x}) = \int_E f_{(n)}(\boldsymbol{x}')[1 + \frac{c^2q^2}{4n-2}\nabla^2]\frac{\mathcal{G}(\boldsymbol{x}-\boldsymbol{x}')}{8\pi\mu}dA(\boldsymbol{x}') , \qquad (3.17)$$

then

$$\boldsymbol{J}_{n+1}(\boldsymbol{x};1) = (2n+1)\int_0^1 u^{2n}\boldsymbol{J}_n(\boldsymbol{x};u)du \quad n = 1,2,3,\ldots , \qquad (3.18)$$

where again the parameter u denotes that the ellipsoid dimensions have been rescaled by u. The derivation is analogous to the discussion subsequent to Equation 3.8.

[1] See his equations (26) and (27). For $c = 0$, the ellipsoid degenerates into an elliptical disk, so $f_1(\boldsymbol{x}')$ is identically the sum of the surface tractions on the two faces of this disk and his identities apply.

The same procedure applied to the right-hand side of Equation 3.16 gives, since $D^2(u) = u^2 D^2(1)$,

$$\begin{aligned}
&\int_0^1 u^{2n} \sum_{k=1}^{\infty} \frac{2^n (k+n-1)!\; D^{2k-2}(u)}{(k-1)!\;(2k+2n-2)!} du \\
&= \sum_{k=1}^{\infty} \frac{2^n (k+n-1)!\; D^{2k-2}}{(k-1)!\;(2k+2n-2)!} \int_0^1 u^{2n+2k-2} du \\
&= \sum_{k=1}^{\infty} \frac{2^{n+1} (k+n)!\; D^{2k-2}}{(k-1)!\;(2k+2n)!} \\
&= \left(\frac{1}{D}\frac{\partial}{\partial D}\right)^n \left(\frac{\sinh D}{D}\right) ,
\end{aligned}$$

as required. The final result for the multipole expansion is given in Table 3.2.

3.3.4 Singularity System for Prolate Spheroids

For ellipsoids of revolution, most of the expressions in the preceding discussions reduce to much simpler forms. The elliptic integrals reduce to more elementary functions, and the axisymmetry may be exploited to simplify the relations between the multipole moments and particle motions. We defer the general discussion on the role of axisymmetry to a later section, but this discussion will furnish examples for later use. We will consider the prolate spheroid ($a > b = c$) here. Oblate spheroids, with $a = b > c$, will be considered in the following subsection.

The ellipsoidal harmonics in the solutions of Oberbeck, Edwardes, and Jeffery are now *spheroidal harmonics.* The relation between our G_n and the standard notation for spheroidal harmonics may be established without great difficulty (Exercise 3.3), but this will not be of further use to us. Instead, we shall focus our attention on the rather interesting simplifications that occur in the singularity and multipole solutions. Prolate spheroids become slender bodies in the limit $c/a \ll 1$, and these exact solutions shall prove quite useful in our discussion of *slender body theory* (Section 3.4).

For a prolate spheroid, the focal ellipse $E(\boldsymbol{x}')$ is degenerate; it is the line segment between the foci of the generating ellipse. The reduction of the image system of the ellipsoid can be achieved by letting $b_E \to 0$ and by taking the Taylor series of $\mathcal{G}(\boldsymbol{x} - \boldsymbol{x}')$ with respect to y' about $y' = 0$ (see Exercise 3.4). Then the integrals in the singularity solution simplify to a line distribution of the form

$$\begin{aligned}
\boldsymbol{J}_n(\boldsymbol{x}) &= \frac{(2n-1)!}{[2^{n-1}(n-1)!]^2} \int_{-ae}^{ae} \left(1 - \frac{x^2}{a^2 e^2}\right)^{n-1} \left[1 + \frac{c^2 \nabla^2}{4n}\right] \frac{\mathcal{G}(\boldsymbol{x} - \boldsymbol{\xi})}{8\pi\mu} \frac{d\xi}{2ae} , \\
&\qquad n = 1, 2, \ldots ,
\end{aligned}$$

where $e = (a^2 - c^2)^{1/2}/a$ is the eccentricity of the generating ellipse.

The multipole expansions in Table 3.2 may be simplified by using the relation

$$\begin{aligned} D^2 &= a^2\frac{\partial}{\partial x^2} + c^2\left(\frac{\partial}{\partial y^2} + \frac{\partial}{\partial z^2}\right) \\ &= (a^2 - c^2)\frac{\partial}{\partial x^2} + c^2\nabla^2 \\ &= D_x^2 + c^2\nabla^2 \,, \end{aligned}$$

with the last equality defining D_x^2. The differential operators that appear in the multipole solution can then be combined into two groups, as shown in the following equation:

$$\begin{aligned} \left(\frac{1}{D}\frac{\partial}{\partial D}\right)^n\left(\frac{\sinh D}{D}\right) &= \left(\frac{1}{D_x}\frac{\partial}{\partial D_x}\right)^n\left(\frac{\sinh D_x}{D_x}\right) \\ &+ \left(\frac{1}{D_x}\frac{\partial}{\partial D_x}\right)^{n+1}\left(\frac{\sinh D_x}{D_x}\right)\frac{c^2}{2}\nabla^2 \,. \end{aligned}$$

Here as before, the operator identity is restricted to operations on biharmonic functions. Consequently, the multipole solutions may be written solely in terms of $\mathcal{G}$ and $\nabla^2\mathcal{G}$ and their derivatives along the axial direction. Thus for the three solutions of greatest interest, we have

$$\begin{aligned} \boldsymbol{v} - \boldsymbol{U}_i^\infty &= -\boldsymbol{F}\cdot\left(\frac{\sinh D_x}{D_x}\right)\frac{\mathcal{G}(\boldsymbol{x})}{8\pi\mu} \\ &\quad - \boldsymbol{F}\cdot\left(\frac{1}{D_x}\frac{\partial}{\partial D_x}\right)\left(\frac{\sinh D_x}{D_x}\right)\frac{c^2}{2}\nabla^2\frac{\mathcal{G}(\boldsymbol{x})}{8\pi\mu} \end{aligned}$$

$$\begin{aligned} \boldsymbol{v} &= \boldsymbol{\Omega}^\infty\times\boldsymbol{x} + \boldsymbol{E}^\infty\cdot\boldsymbol{x} \\ &+ (\boldsymbol{S}\cdot\nabla + \frac{1}{2}\boldsymbol{T}\times\nabla)\cdot\left[\left(\frac{3}{D_x}\frac{\partial}{\partial D_x}\right)\left(\frac{\sinh D_x}{D_x}\right)\frac{\mathcal{G}(\boldsymbol{x})}{8\pi\mu}\right. \\ &\quad \left. + \left(\frac{1}{D_x}\frac{\partial}{\partial D_x}\right)^2\left(\frac{\sinh D_x}{D_x}\right)\frac{3c^2}{2}\frac{\nabla^2\mathcal{G}(\boldsymbol{x})}{8\pi\mu}\right] \,. \end{aligned}$$

The final task is to relate the force, torque, and stresslet on the spheroid to $\boldsymbol{U}^\infty - \boldsymbol{U}$, $\boldsymbol{\Omega}^\infty - \boldsymbol{\omega}$, and $\boldsymbol{E}$. The expressions for the force, torque, and stresslet may be written in a way that highlights the orientation of the various vectors and tensors with respect to the symmetry axis. Denoting the unit directional vector along the axis by $\boldsymbol{d}$, we have

$$\begin{aligned} F_i &= 6\pi\mu a\left[X^A d_i d_j + Y^A(\delta_{ij} - d_i d_j)\right](U_j^\infty - U_j) \\ T_i &= 8\pi\mu a^3\left[X^C d_i d_j + Y^C(\delta_{ij} - d_i d_j)\right](\Omega_j^\infty - \omega_j) \\ &\quad - 8\pi\mu a^3 Y^H\epsilon_{ijl}d_l d_k E_{jk}^\infty \\ S_{ij} &= \frac{20}{3}\pi\mu a^3\left[X^M d_{ijkl}^{(0)} + Y^M d_{ijkl}^{(1)} + Z^M d_{ijkl}^{(2)}\right]E_{kl}^\infty \\ &\quad + \frac{20}{3}\pi\mu a^3\frac{3}{5}Y^H(\epsilon_{ikl}d_j + \epsilon_{jkl}d_i)d_l(\Omega_k^\infty - \omega_k) \,, \end{aligned}$$

where

$$
\begin{aligned}
d^{(0)} &= \frac{3}{2}(d_i d_j - \frac{1}{3}\delta_{ij})(d_k d_l - \frac{1}{3}\delta_{kl}) \\
d^{(1)} &= \frac{1}{2}(d_i\delta_{jl}d_k + d_j\delta_{il}d_k + d_i\delta_{jk}d_l + d_j\delta_{ik}d_l - 4d_i d_j d_k d_l) \\
d^{(2)} &= \frac{1}{2}(\delta_{ik}\delta_{jl} + \delta_{jk}\delta_{il} - \delta_{ij}\delta_{kl} + d_i d_j\delta_{kl} + \delta_{ij}d_k d_l \\
&\quad - d_i\delta_{jl}d_k - d_j\delta_{il}d_k - d_i\delta_{jk}d_l - d_j\delta_{ik}d_l + d_i d_j d_k d_l) \ ,
\end{aligned}
$$

and X, Y, and Z are scalar resistance functions. The X functions are associated with axisymmetric problems, *e.g.*, X^A is used for the force due to translation along the axis of symmetry. Further details and explanations are furnished in Section 3.5.4. The expressions for the scalar functions of the prolate spheroid are given in Table 3.4.

Example 3.3 A Torque-Free Prolate Spheroid in a Linear Field. We use the results for the resistance functions to obtain an important result concerning the angular velocity of a torque-free spheroid in the linear field, $\boldsymbol{\Omega}^\infty \times \boldsymbol{x} + \boldsymbol{E}^\infty \cdot \boldsymbol{x}$. In the expression for the torque, we simply set $\boldsymbol{T} = \boldsymbol{0}$, and dot multiply through with the dyad,

$$
(8\pi\mu a^3)^{-1}\left[(X^C)^{-1}\boldsymbol{dd} + (Y^C)^{-1}(\boldsymbol{\delta} - \boldsymbol{dd})\right]
$$

to obtain

$$
\begin{aligned}
\omega_m - \Omega_m^\infty &= -\left[(X^C)^{-1}d_m d_i + (Y^C)^{-1}(\delta_{mi} - d_m d_i)\right] Y^H \epsilon_{ijl} d_l d_k E_{jk}^\infty \\
&= -(Y^H/Y^C)\epsilon_{mjl}d_l d_k E_{jk}^\infty \ .
\end{aligned}
$$

Using the relation,

$$
\frac{Y^H}{Y^C} = \frac{a^2 - b^2}{a^2 + b^2} \ ,
$$

we find that the rotational motion follows as

$$
\boldsymbol{\omega} \times \boldsymbol{x} = \boldsymbol{\Omega}^\infty \times \boldsymbol{x} + \left(\frac{a^2 - b^2}{a^2 + b^2}\right)\left(\boldsymbol{E}^\infty \cdot \boldsymbol{d}(\boldsymbol{d}\cdot\boldsymbol{x}) - \boldsymbol{E}^\infty : \boldsymbol{dxd}\right) \ .
$$

In words, a prolate spheroid rotates with the angular velocity of the ambient fluid, plus a contribution from the rate-of-strain field, which acts to align the axis along a principal direction of $\boldsymbol{E}$. The relative importance of the alignment effect depends on the aspect ratio: It is most important for slender spheroids, less important for nearly spherical spheroids, and nonexistent for spheres. In Chapter 5, we will study this problem in more detail and show that as the spheroid rotates in the linear field, its axis traces a periodic trajectory known as a *Jeffery orbit.*$\diamondsuit$

$$
\begin{aligned}
F_i &= 6\pi\mu a \left[X^A d_i d_j + Y^A(\delta_{ij} - d_i d_j)\right](U_j^\infty - U_j) \\
T_i &= 8\pi\mu a^3 \left[X^C d_i d_j + Y^C(\delta_{ij} - d_i d_j)\right](\Omega_j^\infty - \omega_j) \\
&\quad - 8\pi\mu a^3 Y^H \epsilon_{ijl} d_l d_k E_{jk}^\infty \\
S_{ij} &= \frac{20}{3}\pi\mu a^3 \left[X^M d_{ijkl}^{(0)} + Y^M d_{ijkl}^{(1)} + Z^M d_{ijkl}^{(2)}\right] E_{kl}^\infty \\
&\quad + \frac{20}{3}\pi\mu a^3 \frac{3}{5} Y^H (\epsilon_{ikl} d_j + \epsilon_{jkl} d_i) d_l (\Omega_k^\infty - \omega_k)
\end{aligned}
$$

$$
\begin{aligned}
d^{(0)} &= \frac{3}{2}(d_i d_j - \frac{1}{3}\delta_{ij})(d_k d_l - \frac{1}{3}\delta_{kl}) \\
d^{(1)} &= \frac{1}{2}(d_i \delta_{jl} d_k + d_j \delta_{il} d_k + d_i \delta_{jk} d_l + d_j \delta_{ik} d_l - 4 d_i d_j d_k d_l) \\
d^{(2)} &= \frac{1}{2}(\delta_{ik}\delta_{jl} + \delta_{jk}\delta_{il} - \delta_{ij}\delta_{kl} + d_i d_j \delta_{kl} + \delta_{ij} d_k d_l \\
&\quad - d_i \delta_{jl} d_k - d_j \delta_{il} d_k - d_i \delta_{jk} d_l - d_j \delta_{ik} d_l + d_i d_j d_k d_l)
\end{aligned}
$$

$$
\begin{aligned}
X^A &= \frac{8}{3} e^3 \left[-2e + (1+e^2)L\right]^{-1} \\
Y^A &= \frac{16}{3} e^3 \left[2e + (3e^2 - 1)L\right]^{-1} \\
X^C &= \frac{4}{3} e^3 (1 - e^2) \left[2e - (1 - e^2)L\right]^{-1} \\
Y^C &= \frac{4}{3} e^3 (2 - e^2) \left[-2e + (1 + e^2)L\right]^{-1} \\
Y^H &= \frac{4}{3} e^5 \left[-2e + (1 + e^2)L\right]^{-1} \\
X^M &= \frac{8}{15} e^5 \left[(3 - e^2)L - 6e\right]^{-1} \\
Y^M &= \frac{4}{5} e^5 \left[2e(1 - 2e^2) - (1 - e^2)L\right] \\
&\quad \times \left[\left(2e(2e^2 - 3) + 3(1 - e^2)L\right)\left(-2e + (1 + e^2)L\right)\right]^{-1} \\
Z^M &= \frac{16}{5} e^5 (1 - e^2) \left[3(1 - e^2)^2 L - 2e(3 - 5e^2)\right]^{-1} \\
L(e) &= \ln\left(\frac{1+e}{1-e}\right)
\end{aligned}
$$

Table 3.4: The *resistance functions* for the prolate spheroid.

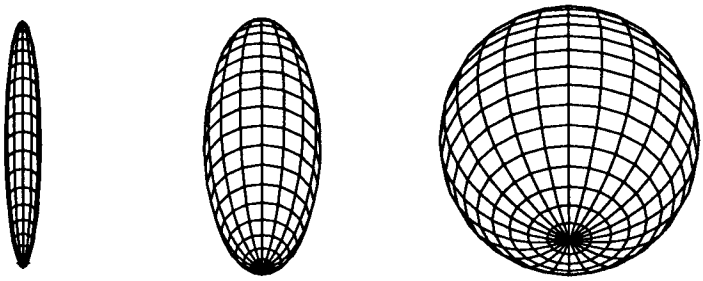

Figure 3.1: Prolate spheroids of various aspect ratios.

	$e \ll 1$	Needles: $\epsilon = \sqrt{1-e^2} \ll 1, \quad E = (\ln(2/\epsilon))^{-1}$
X^A	$1 - \frac{2e^2}{5} - \frac{17e^4}{175} + \cdots$	$\frac{4E}{6-3E} - \frac{(8-6E)E\epsilon^2}{12-12E+3E^2} + \cdots$
Y^A	$1 - \frac{3e^2}{10} - \frac{57e^4}{700} + \cdots$	$\frac{8E}{6+3E} - \frac{4E^2\epsilon^2}{12+12E+3E^2} + \cdots$
X^C	$1 - \frac{6e^2}{5} + \frac{27e^4}{175} + \cdots$	$\frac{2\epsilon^2}{3} + \frac{(2-2E)\epsilon^4}{3E} + \cdots$
Y^C	$1 - \frac{9e^2}{10} + \frac{18e^4}{175} + \cdots$	$\frac{2E}{6-3E} + \frac{E^2\epsilon^2}{12-12E+3E^2} + \cdots$
Y^H	$\frac{e^2}{2} - \frac{e^4}{5} + \cdots$	$\frac{2E}{6-3E} - \frac{(8-5E)E\epsilon^2}{12-12E+3E^2} + \cdots$
X^M	$1 - \frac{6e^2}{7} - \frac{e^4}{49} + \cdots$	$\frac{4E}{30-45E} - \frac{(24-26E)E\epsilon^2}{60-180E+135E^2} + \cdots$
Y^M	$1 - \frac{13e^2}{14} + \frac{44e^4}{735} + \cdots$	$\frac{2E}{10-5E} - \frac{(16-32E+13E^2)\epsilon^2}{20-20E+5E^2} + \cdots$
Z^M	$1 - \frac{8e^2}{7} + \frac{17e^4}{147} + \cdots$	$\frac{4\epsilon^2}{5} + \frac{2\epsilon^4}{5} + \cdots$

Table 3.5: Asymptotic behavior of the resistance functions for prolate spheroids: near-spheres ($e \ll 1$) and needles ($e \to 1$).

3.3.5 Singularity System for Oblate Spheroids

For an oblate spheroid ($a = b > c$), the focal ellipse $E(\boldsymbol{x}')$ becomes a circular disk of radius $a_E = b_E = ae$. Now consider the relation

$$\begin{aligned} D^2 &= a^2\left(\frac{\partial}{\partial x^2}+\frac{\partial}{\partial y^2}\right)+c^2\frac{\partial}{\partial z^2} \\ &= -(a^2-c^2)\frac{\partial}{\partial z^2}+a^2\nabla^2 \\ &= -D_z^2+a^2\nabla^2 \,. \end{aligned}$$

We see, by comparing this result with the earlier one for prolate spheroids, that the multipole expansion for the oblate spheroid can be obtained from that for the prolate spheroid by replacing D_x with iD_z and $c^2\nabla^2$ with $a^2\nabla^2$. Therefore, the multipole expansion for the oblate spheroid simplifies as follows:

$$\begin{aligned} \left(\frac{1}{D}\frac{\partial}{\partial D}\right)^n\left(\frac{\sinh D}{D}\right) &= \left(\frac{-1}{D_z}\frac{\partial}{\partial D_z}\right)^n\left(\frac{\sin D_z}{D_z}\right) \\ &\quad+\left(\frac{-1}{D_z}\frac{\partial}{\partial D_z}\right)^{n+1}\left(\frac{\sin D_z}{D_z}\right)\frac{a^2}{2}\nabla^2 \,, \end{aligned}$$

where, as before, the operator identity is restricted to operations on biharmonic functions. Again, the solutions are expressed in terms of $\mathcal{G}$ and $\nabla^2\mathcal{G}$ and their derivatives along the axial direction. Thus for the three solutions of greatest interest, we have

$$\begin{aligned} \boldsymbol{v}-\boldsymbol{U}_i^\infty &= -\boldsymbol{F}\cdot\left(\frac{\sin D_z}{D_z}\right)\frac{\mathcal{G}(\boldsymbol{x})}{8\pi\mu} \\ &\quad+\boldsymbol{F}\cdot\left(\frac{1}{D_z}\frac{\partial}{\partial D_z}\right)\left(\frac{\sin D_z}{D_z}\right)\frac{a^2}{2}\nabla^2\frac{\mathcal{G}(\boldsymbol{x})}{8\pi\mu} \end{aligned}$$

$$\begin{aligned} \boldsymbol{v} &= \boldsymbol{\Omega}^\infty\times\boldsymbol{x}+\boldsymbol{E}^\infty\cdot\boldsymbol{x} \\ &\quad+(\boldsymbol{S}\cdot\nabla+\frac{1}{2}\boldsymbol{T}\times\nabla)\cdot\left[\left(\frac{-3}{D_z}\frac{\partial}{\partial D_z}\right)\left(\frac{\sin D_z}{D_z}\right)\frac{\mathcal{G}(\boldsymbol{x})}{8\pi\mu}\right. \\ &\quad\left.+\left(\frac{1}{D_z}\frac{\partial}{\partial D_z}\right)^2\left(\frac{\sin D_z}{D_z}\right)\frac{3a^2}{2}\frac{\nabla^2\mathcal{G}(\boldsymbol{x})}{8\pi\mu}\right] . \end{aligned}$$

The force, torque, and stresslet on the oblate spheroid are also written in terms of $\boldsymbol{d}$ and the scalar functions X, Y, and Z (see Table 3.6). The expressions for the oblate and prolate ellipsoids of revolution are closely related. In fact, each resistance function for one may be obtained from the counterpart of the other by replacing e with $ie/\sqrt{1-e^2}$. This is equivalent to switching the roles played by a and c (see Exercise 3.5).

The multipole expansion is the appropriate form when $|\boldsymbol{x}| \gg a$, but does it converge for $|\boldsymbol{x}| \sim c$? To answer this question, let us consider the disturbance

field of an oblate spheroid translating in the direction of its axis and examine $\boldsymbol{v}(\boldsymbol{x}_1)$ for points $\boldsymbol{x}_1$ on the axis of symmetry. We use the following identities derived with the help of formulae linking Stokes multipoles to the spherical harmonics (see Section 4.2.1):

$$\begin{aligned}\frac{(\boldsymbol{d}\cdot\nabla)^n}{n!}\boldsymbol{F}^{\parallel}\cdot\mathcal{G}(\boldsymbol{x})|_{x=x_1} &= 2\boldsymbol{F}^{\parallel}r^{-(n+1)}\\ \frac{(\boldsymbol{d}\cdot\nabla)^n}{n!}\boldsymbol{F}^{\parallel}\cdot\nabla^2\mathcal{G}(\boldsymbol{x})|_{x=x_1} &= -2(n+1)(n+2)\boldsymbol{F}^{\parallel}r^{-(n+3)}\ ,\end{aligned}$$

where $r=|\boldsymbol{x}_1|$, $\boldsymbol{d}=\boldsymbol{x}_1/r$ and $\boldsymbol{F}^{\parallel}$ is used to denote that $\boldsymbol{F}$ is parallel to $\boldsymbol{d}$. If we insert these results into the multipole expansion, we obtain

$$\boldsymbol{v}(\boldsymbol{x}_1)=-\frac{\boldsymbol{F}^{\parallel}}{8\pi\mu}\frac{3}{2}\frac{a}{r}\sum_{k=0}^{\infty}(-1)^k\left[\frac{1}{2k+1}-\frac{a^2}{r^2}\frac{k+1}{2k+3}\right]\left(\frac{a_E}{r}\right)^{2k}\ .$$

The infinite series in r^{-1} converges only if $r^{-1}\le a_E=ae$. We may visualize this constraint as a "hemispheric dome" of radius ae over the focal circle of the spheroid. As we slide down the axis of symmetry toward the spheroid, the infinite series will converge only if $\boldsymbol{x}_1$ lies outside the hemisphere. This example thus illustrates that, in general, the multipole expansion has a finite radius of convergence in r^{-1}, and that the exact value of this radius of convergence depends on the details of the particle geometry. In particular, it need not correspond to the particle surface nor the surface of an "effective sphere" that circumscribes the particle.

For translations transverse to the axis, we use

$$\begin{aligned}\frac{(\boldsymbol{d}\cdot\nabla)^n}{n!}\boldsymbol{F}^{\perp}\cdot\mathcal{G}(\boldsymbol{x})|_{x=x_1} &= \boldsymbol{F}^{\perp}r^{-(n+1)}\\ \frac{(\boldsymbol{d}\cdot\nabla)^n}{n!}\boldsymbol{F}^{\perp}\cdot\nabla^2\mathcal{G}(\boldsymbol{x})|_{x=x_1} &= (n+1)(n+2)\boldsymbol{F}^{\perp}r^{-(n+3)}\end{aligned}$$

to obtain the corresponding result,

$$\boldsymbol{v}(\boldsymbol{x}_1)=\frac{\boldsymbol{F}^{\perp}}{8\pi\mu}\frac{3}{4}\frac{a}{r}\sum_{k=0}^{\infty}(-1)^k\left[\frac{1}{2k+1}+\frac{a^2}{r^2}\frac{k+1}{2k+3}\right]\left(\frac{a_E}{r}\right)^{2k}\ .$$

Again, the radius of convergence is at $r^{-1}=ae$. Similar results hold for the prolate spheroid.

3.4 Slender Body Theory

Consider a needle-like rigid body whose length $2a$ is much greater than its width $2b$. Such particles are encountered in many settings, such as pulp fibers, rigid biopolymers like the tobacco mosaic virus, and various metal oxides used in the manufacture of magnetic storage devices. Understanding the motion of such particles in a viscous fluid is therefore of some importance.

$$
\begin{aligned}
F_i &= 6\pi\mu a \left[X^A d_i d_j + Y^A(\delta_{ij} - d_i d_j)\right](U_j^\infty - U_j) \\
T_i &= 8\pi\mu a^3 \left[X^C d_i d_j + Y^C(\delta_{ij} - d_i d_j)\right](\Omega_j^\infty - \omega_j) \\
&\quad - 8\pi\mu a^3 Y^H \epsilon_{ijl} d_l d_k E_{jk}^\infty \\
S_{ij} &= \frac{20}{3}\pi\mu a^3 \left[X^M d_{ijkl}^{(0)} + Y^M d_{ijkl}^{(1)} + Z^M d_{ijkl}^{(2)}\right] E_{kl}^\infty \\
&\quad + \frac{20}{3}\pi\mu a^3 \frac{3}{5} Y^H (\epsilon_{ikl} d_j + \epsilon_{jkl} d_i) d_l (\Omega_k^\infty - \omega_k)
\end{aligned}
$$

$$
\begin{aligned}
d^{(0)} &= \frac{3}{2}(d_i d_j - \frac{1}{3}\delta_{ij})(d_k d_l - \frac{1}{3}\delta_{kl}) \\
d^{(1)} &= \frac{1}{2}(d_i\delta_{jl}d_k + d_j\delta_{il}d_k + d_i\delta_{jk}d_l + d_j\delta_{ik}d_l - 4d_i d_j d_k d_l) \\
d^{(2)} &= \frac{1}{2}(\delta_{ik}\delta_{jl} + \delta_{jk}\delta_{il} - \delta_{ij}\delta_{kl} + d_i d_j \delta_{kl} + \delta_{ij} d_k d_l \\
&\quad - d_i\delta_{jl}d_k - d_j\delta_{il}d_k - d_i\delta_{jk}d_l - d_j\delta_{ik}d_l + d_i d_j d_k d_l) \ ,
\end{aligned}
$$

$$
\begin{aligned}
X^A &= \frac{4}{3}e^3 \left[(2e^2-1)C + e\sqrt{1-e^2}\right]^{-1} \\
Y^A &= \frac{8}{3}e^3 \left[(2e^2+1)C - e\sqrt{1-e^2}\right]^{-1} \\
X^C &= \frac{2}{3}e^3 \left[C - e\sqrt{1-e^2}\right]^{-1} \\
Y^C &= \frac{2}{3}e^3(2-e^2) \left[e\sqrt{1-e^2} - (1-2e^2)C\right]^{-1} \\
Y^H &= -\frac{2}{3}e^5 \left[e\sqrt{1-e^2} - (1-2e^2)C\right]^{-1} \\
X^M &= \frac{4}{15}e^5 \left[(3-2e^2)C - 3e\sqrt{1-e^2}\right]^{-1} \\
Y^M &= \frac{2}{5}e^5 \left[e(1+e^2) - \sqrt{1-e^2}C\right] \\
&\quad \times \left[\left(3e - e^3 - 3\sqrt{1-e^2}C\right)\left(e\sqrt{1-e^2} - (1-2e^2)C\right)\right]^{-1} \\
Z^M &= \frac{8}{5}e^5 \left[3C - (2e^3+3e)\sqrt{1-e^2}\right]^{-1} \\
C(e) &= \cot^{-1}\left(\frac{\sqrt{1-e^2}}{e}\right)
\end{aligned}
$$

Table 3.6: The *resistance functions* for the oblate spheroid.

Figure 3.2: Oblate spheroids of various aspect ratios.

	$e \ll 1$	Disks: $\epsilon = \sqrt{1-e^2} \ll 1$
X^A	$1 - \frac{e^2}{10} - \frac{31e^4}{1400} + \cdots$	$\frac{8}{3\pi}(1 + \frac{1}{2}\epsilon^2 + \cdots)$
Y^A	$1 - \frac{e^2}{5} - \frac{79e^4}{1400} + \cdots$	$\frac{16}{9\pi}(1 + \frac{8}{3\pi}\epsilon - \frac{15\pi^2-128}{18\pi^2}\epsilon^2 + \cdots)$
X^C	$1 - \frac{3e^2}{10} - \frac{99e^4}{1400} + \cdots$	$\frac{4}{3\pi}(1 + \frac{4}{\pi}\epsilon + \frac{32-3\pi^2}{2\pi^2}\epsilon^2 + \cdots)$
Y^C	$1 - \frac{3e^2}{5} + \frac{39e^4}{1400} + \cdots$	$\frac{4}{3\pi}(1 + \frac{3}{2}\epsilon^2 + \cdots)$
Y^H	$-\frac{1}{2}e^2(1 - \frac{e^2}{10} - \frac{31e^4}{1400} + \cdots)$	$-\frac{4}{3\pi}(1 - \frac{1}{2}\epsilon^2 + \cdots)$
X^M	$1 - \frac{9e^2}{14} - \frac{13e^4}{392} + \cdots$	$\frac{8}{15\pi}(1 + \frac{8}{\pi}\epsilon + \frac{128-9\pi^2}{2\pi^2}\epsilon^2 + \cdots)$
Y^M	$1 - \frac{4e^2}{7} - \frac{173e^4}{5880} + \cdots$	$\frac{4}{5\pi}(1 + \frac{\pi}{2}\epsilon + \frac{3\pi^2-20}{8}\epsilon^2 + \cdots)$
Z^M	$1 - \frac{5e^2}{14} - \frac{95e^4}{1176} + \cdots$	$\frac{16}{15\pi}(1 + \frac{16}{3\pi}\epsilon + \frac{512-45\pi^2}{18\pi^2}\epsilon^2 + \cdots)$

Table 3.7: Asymptotic behavior of the resistance functions for oblate spheroids: near-spheres ($e \ll 1$) and disks ($e \to 1$).

Let $\boldsymbol{x}$ represent a point in the fluid, the origin taken at the particle center. For $|\boldsymbol{x}| \gg a$, we obtain the usual result: The exact shape and overall dimensions of the particle are not important and the disturbance field is described accurately by a multipole expansion about the origin. The Stokeslet and rotlet fields account for the force and torque on the particle and the stresslet field describes the effect of the particle on the rate-of-strain in the fluid. Higher order multipoles contribute ever smaller corrections, their influence diminishing by factors of $a/|\boldsymbol{x}|$. On the other hand, for $|\boldsymbol{x}|$ less than a, the details concerning the shape of the particle, specifically the overall length, is clearly important and an expansion about the particle center no longer makes any sense; in fact, we learned earlier in this chapter that these expansions can be nonconvergent near the particle.

Recall that the multipole expansion originates from the integral representation for the disturbance field. The idea was that at great distances from the particle, the surface distribution of Stokeslets is expanded in a Taylor series about the particle center. For a slender body, we instead expand the Stokeslets about points on the particle axis, thus taking advantage of the "smallness" of b. The result is a line distribution of the lower order singularities, much like those encountered for prolate spheroids.

Burgers [19] gave an elementary version of this idea and correctly deduced that, to leading order, the disturbance field of a slender body in uniform translation is given by a constant line distribution of Stokeslets over the particle length. The field was revived in the 1960s [17, 18, 84, 87] and placed on a more rigorous foundation using the theory of matched asymptotic expansions [86]. The theory has been generalized in a number of directions, for example, noncircular cross sections [5], more general ambient fields [5, 23, 47], and center-line curvature [47]. In this introduction, we consider only the simplest case of a slender body of circular cross section and straight backbone (*i.e.*, an axisymmetric particle). Nevertheless, the solution will be general in that explicit formulae will be obtained for particles of arbitrary shape, save for the slenderness condition.

The development of the theory for inviscid potential flow preceded, and thus influenced, the development of the theory for Stokes flow. This has led to some unfortunate consequences, such as the use of singularities from potential flow, with the result that some of the unifying structures are obscured. For example, the solutions for translations parallel to and transverse to the axis are actually quite similar when represented in terms of Stokes singularities, but appear quite different when written in terms of singularities from potential flow. For this reason, we have rewritten the solutions here in terms of $\mathcal{G}$ and its derivatives, but they may be derived by a formal procedure analogous to that in Tillett [86].

The geometry of this problem is given in the Figure 3.3 We place the particle along the x-axis, with the particle shape described by the cylindrical radial coordinate, ρ:

$$\rho(x) = \sqrt{y^2 + z^2} = \epsilon R(x) \qquad -a \leq x \leq a \ .$$

Since $\epsilon = b/a \ll 1$ has been scaled from the width, $max\{R(x)\} = a$. The ends

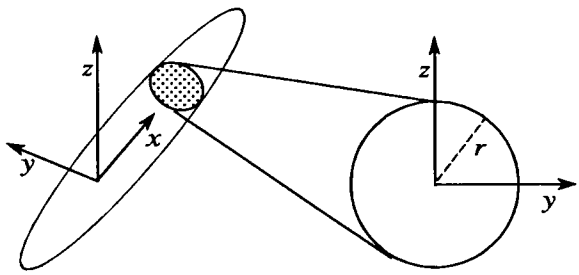

Figure 3.3: The geometry of the slender body.

are assumed to be round, with $R^2 \sim A^+(a-x)$ near $x = a$ and $R^2 \sim A^-(a+x)$ near $x = -a$. For the prolate spheroid, $A^+ = A^- = 2a$.

Consider a slender body in steady translation through a quiescent fluid. We obtain the leading order terms of slender body theory by following the exposition in [5]. Consider the velocity field produced by a constant line distribution of Stokeslets,

$$v_i = f_j \int_{-a}^{a} \frac{\mathcal{G}_{ij}(\boldsymbol{x} - \boldsymbol{\xi})}{8\pi\mu}\, d\xi \ .$$

With $\boldsymbol{\xi}$ on the x-axis, the nine components of the dyadic integral are

$$\begin{pmatrix} I + \mathcal{I}_2 & \mathcal{I}_1 \cos\phi & \mathcal{I}_1 \sin\phi \\ \mathcal{I}_1 \cos\phi & I + \mathcal{I}_0 \cos^2\phi & \mathcal{I}_0 \sin\phi\cos\phi \\ \mathcal{I}_1 \sin\phi & \mathcal{I}_0 \sin\phi\cos\phi & I + \mathcal{I}_0 \sin^2\phi \end{pmatrix} ,$$

where I and $\mathcal{I}_n$ are elementary integrals defined by

$$I = \int_{-a}^{a} \frac{d\xi}{\{(x-\xi)^2 + \rho^2\}^{1/2}} \ , \qquad \mathcal{I}_n = \int_{-a}^{a} \frac{\rho^{2-n}(x-\xi)^n\, d\xi}{\{(x-\xi)^2 + \rho^2\}^{3/2}} \ .$$

For $\rho \sim b \ll a$, these integrals take the asymptotic values,

$$I \sim 2\ln(2/\epsilon) + O(\epsilon^2) = 2E^{-1} + O(\epsilon^2) \ ,$$

$$\mathcal{I}_0 \sim 2 + O(\epsilon^2) \ , \quad \mathcal{I}_1 \sim O(\epsilon^2) \ , \quad \mathcal{I}_2 \sim 2E^{-1} - 2 + O(\epsilon^2) \ ,$$

and the dyadic integral becomes, to $O(\epsilon^2)$,

$$\begin{pmatrix} 4E^{-1} - 2 & 0 & 0 \\ 0 & 2E^{-1} + 2\cos^2\phi & 2\sin\phi\cos\phi \\ 0 & 2\sin\phi\cos\phi & 2E^{-1} + 2\sin^2\phi \end{pmatrix} .$$

For convenience, we have defined the small parameter $E = 1/\ln(2/\epsilon)$. Thus for $\rho \ll a$ (and provided also that we are away from the ends) the velocity field is a constant of the form

$$\boldsymbol{v} \sim \frac{1}{4\pi\mu E} \boldsymbol{f} \cdot [2\boldsymbol{dd} + (\boldsymbol{\delta} - \boldsymbol{dd}) + O(E)] \ ,$$

and thus describes a rigid translation of the slender body. This suggests that for a slender body translating with a velocity $\boldsymbol{U}$, the disturbance field is approximately that produced by a line distribution of Stokeslets, with a constant force density given by

$$\begin{aligned} f^{\parallel} &= 2\pi\mu E U^{\parallel} + O(E^2) \\ f^{\perp} &= 4\pi\mu E U^{\perp} + O(E^2) \ . \end{aligned}$$

The drag on the particle is simply the net Stokeslet strength obtained by integration over the axis,

$$\begin{aligned} F^{\parallel} &= 4\pi\mu a E U + O(E^2) \\ F^{\perp} &= 8\pi\mu a E U + O(E^2) \ , \end{aligned}$$

and thus we recover Burger's deduction that the drag for axial translation is one-half that for transverse translation.

This simple version of slender body theory may be refined by including higher order singularities and by computing the line integrals to higher order [5, 86]. The singular behavior at the ends is handled by a separate expansion in those regions, following the standard procedure of matched asymptotic analysis [34, 88]. The end result for the disturbance field produced by translation of a slender body may be written as

$$\begin{aligned} \boldsymbol{v} &= -\boldsymbol{U} \cdot \int_{\alpha}^{\beta} \left[f^{\parallel}(\xi)\boldsymbol{dd} + f^{\perp}(\xi)(\boldsymbol{\delta} - \boldsymbol{dd}) \right] \cdot \left\{ 1 + \frac{1}{4}(\epsilon R(\xi))^2 \nabla^2 \right\} \mathcal{G}(\boldsymbol{x} - \boldsymbol{\xi})\, d\xi \\ &+ \int_{\alpha}^{\beta} h(\xi)(\boldsymbol{U} \cdot \nabla)\boldsymbol{d} \cdot \mathcal{G}(\boldsymbol{x} - \boldsymbol{\xi})\, d\xi \ , \end{aligned}$$

with

$$\begin{aligned} f^{\parallel}(\xi) &= \frac{E}{4} \left\{ \frac{1 - E \ln[(a^2 - \xi^2)^{1/2}/R(\xi)]}{1 - \frac{1}{2}E} \right\} + O(1/\ln\epsilon)^3 \\ f^{\perp}(\xi) &= \frac{E}{2} \left\{ \frac{1 - E \ln[(a^2 - \xi^2)^{1/2}/R(\xi)]}{1 + \frac{1}{2}E} \right\} + O(1/\ln\epsilon)^3 \\ h(\xi) &= \frac{1}{4}\epsilon^2 \frac{d}{d\xi} \left(R(\xi)^2 f^{\perp}(\xi) \right) \\ &\quad + \frac{1}{2}(\epsilon R(\xi))^2 \left\{ \frac{d}{d\xi} \left[\left(\ln \left(\frac{(a^2 - \xi^2)^{1/2}}{R(\xi)} \right) + \frac{1}{E} - 1 \right) f^{\perp}(\xi) \right] \right. \\ &\qquad + \frac{R'(\xi)}{R(\xi)} f^{\perp}(\xi) \\ &\quad \left. + \frac{1}{2} \int_{\alpha}^{\beta} \frac{f^{\perp}(\xi) - f^{\perp}(x) - (\xi - x) f^{\perp\prime}(x)}{(\xi - x)^2} \mathrm{sgn}(\xi - x) d\xi \right\} \ . \end{aligned}$$

The disturbance field is represented by a line distribution of Stokeslets, degenerate Stokes quadrupoles, and Stokes dipoles (stresslets and rotlets). In the limit of small b/a, the singularity solution for the prolate spheroid is consistent with that obtained by slender body theory.

By analyzing the asymptotic behavior at the ends, Tillet has shown that the distribution provides a uniform flow near a and $-a$ if the distribution ends at the foci of the osculating spheroid, *i.e.*,

$$\alpha = -a + \frac{1}{4}\epsilon^2 A^- \ , \quad \beta = a - \frac{1}{4}\epsilon^2 A^+ \ .$$

The ratio of the Stokeslet densities for axisymmetric and transverse motions are

$$\frac{f^{\parallel}}{f^{\perp}} = \frac{1}{2}\left(\frac{1+\frac{1}{2}E}{1-\frac{1}{2}E}\right) = \frac{1}{2}(1 + E + \cdots) \ ,$$

so that the drag for axisymmetric motion is one-half that for transverse motions, with a small $(\ln \epsilon^{-1})^{-1}$ correction that is independent of the particle shape.

3.5 Faxén Laws

So far in this chapter, we have discussed various aspects of the multipole expansion and have presented several examples and applications. However, with the exception of a few simple examples (where the solution can be obtained by other means), we have not addressed a key point – a method for determining the multipole moments. Thus, the question is: Given only the ambient flow $\boldsymbol{v}^\infty(\boldsymbol{x})$ and the motion of the particle, how do we determine the moments?

The answer to the question takes the form of direct relations, known as Faxén laws, that express the moments in terms of $\boldsymbol{v}^\infty$ and its derivatives. Actually, Hilding Faxén's original work [28, 29] concerned only the force and torque on a sphere; the original Faxén laws are essentially

$$\boldsymbol{F} = 6\pi\mu a\left(1 + \frac{a^2}{6}\nabla^2\right)\boldsymbol{v}^\infty(\boldsymbol{x})|_{x=0} - 6\pi\mu a\boldsymbol{U} \tag{3.19}$$

$$\boldsymbol{T} = 8\pi\mu a^3(\boldsymbol{\Omega}^\infty(\boldsymbol{x}) - \boldsymbol{\omega})|_{x=0} \ , \tag{3.20}$$

and were derived by calculating the force and torque from Lamb's general solution. Thus Faxén's original approach is not readily extended to the general particle.

The law for the force contains two interesting features. The first is that the correction to Stokes' law required by the general ambient flow $\boldsymbol{v}^\infty$ is relatively simple, being proportional to the ambient pressure gradient $\nabla^2\boldsymbol{v}^\infty = \nabla p^\infty/\mu$. The second, and perhaps the more remarkable, aspect is that we have encountered the grouping $(1 + (a^2/6)\nabla^2)$ before, in our discussion of the singularity solution for the translating sphere. We shall see that this reoccurrence is not accidental, but follows as a corollary to the Lorentz reciprocal theorem. This observation leads to a method for construction of moments for the general particle.

We recall from Chapter 2 the following more general statement of the Lorentz reciprocal theorem:

$$\oint_S \boldsymbol{v}_1 \cdot (\boldsymbol{\sigma}_2 \cdot \boldsymbol{n})\, dS - \int_V \boldsymbol{v}_1 \cdot (\nabla \cdot \boldsymbol{\sigma}_2)\, dV$$

$$= \oint_S \boldsymbol{v}_2 \cdot (\boldsymbol{\sigma}_1 \cdot \boldsymbol{n})\, dS - \int_V \boldsymbol{v}_2 \cdot (\nabla \cdot \boldsymbol{\sigma}_1)\, dV \ , \tag{3.21}$$

where V is the fluid volume bounded by the particle surface and a large sphere "at infinity." The surface integrals are over these boundaries of V. Recall that the simpler and more frequently used form of the reciprocal theorem follows from the assumption $\nabla \cdot \boldsymbol{\sigma} = 0$. We relax this condition here for reasons that will soon become apparent.

In all applications of the reciprocal theorem in this section, the fields $\boldsymbol{v}_1$, $\boldsymbol{\sigma}_1$, $\boldsymbol{v}_2$, and $\boldsymbol{\sigma}_2$ *decay far away from the particle*, to the extent that the surface contributions from S_∞ vanish in the limit of large S_∞. The integral over the particle surface S_p is written in terms of the outward normal (which points into the fluid), so that Equation 3.21 may be rewritten as

$$\begin{aligned} &\oint_{S_p} \boldsymbol{v}_1 \cdot (\boldsymbol{\sigma}_2 \cdot \boldsymbol{n})\, dS + \int_V \boldsymbol{v}_1 \cdot (\nabla \cdot \boldsymbol{\sigma}_2)\, dV \\ &\quad = \oint_{S_p} \boldsymbol{v}_2 \cdot (\boldsymbol{\sigma}_1 \cdot \boldsymbol{n})\, dS + \int_V \boldsymbol{v}_2 \cdot (\nabla \cdot \boldsymbol{\sigma}_1)\, dV \ . \end{aligned} \tag{3.22}$$

Let us now take for $\boldsymbol{v}_1$ the solution for a particle translating with velocity $\boldsymbol{U}$ in a quiescent fluid. We note that $\nabla \cdot \boldsymbol{\sigma}_1 = 0$ in V. For $\boldsymbol{v}_2$, we take the velocity field generated by a point force $\boldsymbol{F} \cdot \mathcal{G}(\boldsymbol{x} - \boldsymbol{y})/8\pi\mu$, where $\boldsymbol{y}$ lies outside the particle, and the particle is stationary. Then $\boldsymbol{v}_2 = 0$ on S_p, and $\nabla \cdot \boldsymbol{\sigma}_2 = -\boldsymbol{F}\delta(\boldsymbol{x} - \boldsymbol{y})$ in V. When these boundary conditions and identities are inserted into Equation 3.22, the result is

$$\boldsymbol{U} \cdot \boldsymbol{F}_2 - \boldsymbol{v}_1(\boldsymbol{y}) \cdot \boldsymbol{F} = 0 \ , \tag{3.23}$$

where $\boldsymbol{F}_2$ is the force on the particle generated by the surface traction $\boldsymbol{\sigma}_2 \cdot \boldsymbol{n}$. Due to linearity of the Stokes equation, we may factor $\boldsymbol{U}$ from $\boldsymbol{v}_1$. Furthermore, suppose that $\boldsymbol{v}_1$ is written as a singularity solution, so that

$$\boldsymbol{v}_1(\boldsymbol{x}) = \boldsymbol{U} \cdot \mathcal{F}\{\mathcal{G}(\boldsymbol{x} - \boldsymbol{\xi})/8\pi\mu\} \ , \tag{3.24}$$

where $\mathcal{F}$ is a linear functional and $\boldsymbol{\xi}$ represents the region inside the translating particle over which the singularities are distributed. Then Equation 3.23 becomes

$$(\boldsymbol{F}_2)_i = \mathcal{F}\{F_j \mathcal{G}_{ji}(\boldsymbol{y} - \boldsymbol{\xi})/8\pi\mu\} \ . \tag{3.25}$$

However, $F_j \mathcal{G}_{ji}(\boldsymbol{y} - \boldsymbol{\xi})/8\pi\mu = F_j \mathcal{G}_{ij}(\boldsymbol{\xi} - \boldsymbol{y})/8\pi\mu$ is[2] the ambient field of the $\boldsymbol{v}_2$ problem, evaluated over the image region, $\boldsymbol{x} = \boldsymbol{\xi}$. So for this case we have shown that

$$\boldsymbol{F}_2 = \mathcal{F}\{\boldsymbol{v}^\infty(\boldsymbol{\xi})\} \ . \tag{3.26}$$

But all ambient fields $\boldsymbol{v}^\infty$ that satisfy the Stokes equation can be constructed from an appropriate set of images, so Equation 3.26 holds for the general ambient field. For spheres, recall $\boldsymbol{\xi}$ is the sphere center and that

$$\mathcal{F} = 6\pi\mu a\{1 + \frac{a^2}{6}\nabla^2\} \ , \tag{3.27}$$

[2]This equality can be verified directly, but it also follows from the self-adjoint property of the Green's dyadic (see Exercise 2.16).

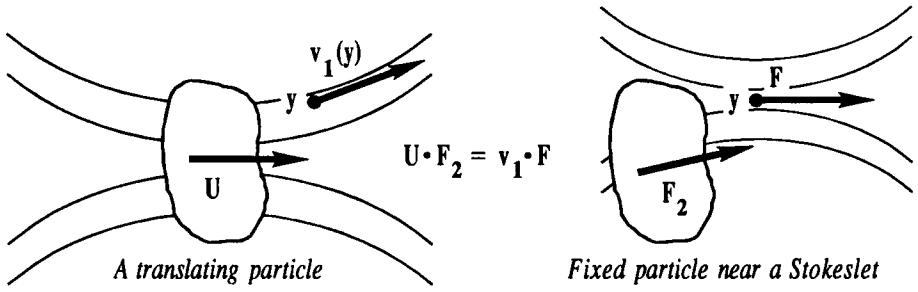

Figure 3.4: A reciprocal relation: the translational disturbance field and the drag on a sphere near a Stokeslet.

so we recover Faxén's original result for the force on the sphere.[3] The analogous development of the Faxén law for the torque and stresslet on a stationary particle yields (see Exercise 3.6)

$$\boldsymbol{T} = \mathcal{T}\{\boldsymbol{v}^{\infty}(\boldsymbol{\xi})\} \tag{3.28}$$

$$\boldsymbol{S} = \mathcal{S}\{\boldsymbol{v}^{\infty}(\boldsymbol{\xi})\} \tag{3.29}$$

where $\mathcal{T}$ and $\mathcal{S}$ are the linear functionals of $\mathcal{G}(\boldsymbol{x}-\boldsymbol{\xi})/8\pi\mu$ associated with the singularity solutions with boundary conditions $\boldsymbol{\omega}\times\boldsymbol{x}$ and $\boldsymbol{E}\cdot\boldsymbol{x}$. The Faxén laws for a moving particle are obtained by adding the contributions for the particle moving through quiescent fluid to the results for the stationary particle.

Example 3.4 The Faxén Laws for the Torque and Stresslet on a Sphere.

We first derive the results for a stationary sphere. The singularity solution for the rotating sphere is

$$v_i = -4\pi\mu a^3 \epsilon_{jk\ell}\omega_\ell \frac{\partial}{\partial \xi_k}\frac{\mathcal{G}_{ij}(\boldsymbol{x}-\boldsymbol{\xi})}{8\pi\mu} ,$$

so that

$$T_\ell = -4\pi\mu a^3 \epsilon_{jk\ell}\frac{\partial v_j^{\infty}}{\partial \xi_k}|_{x=0} = 8\pi\mu a^3 \Omega_\ell^{\infty}(\boldsymbol{x})|_{x=0} .$$

The result for a rotating sphere, Equation 3.20, follows by linear superposition.

The singularity solution for the straining field is

$$v_i = E_{ij}x_j - \frac{20}{3}\pi\mu a^3 E_{jk}\{1+\frac{a^2}{10}\nabla^2\} \times\frac{1}{2}\left(\frac{\partial}{\partial \xi_k}\frac{\mathcal{G}_{ij}(\boldsymbol{x}-\boldsymbol{\xi})}{8\pi\mu} + \frac{\partial}{\partial \xi_j}\frac{\mathcal{G}_{ik}(\boldsymbol{x}-\boldsymbol{\xi})}{8\pi\mu}\right) .$$

[3]This simple derivation was pointed out to us in a private communication from Dr. E.J. Hinch, of Cambridge University.

It is now clear which terms generate $\boldsymbol{E} \cdot \boldsymbol{x}$ on the sphere surface, so that

$$S_{jk} = \frac{20}{3}\pi\mu a^3\{1 + \frac{a^2}{10}\nabla^2\}e_{jk}(\boldsymbol{x})|_{x=0} \ .$$

The stresslet on a sphere in an arbitrary field is the sum of two contributions: an ambient rate-of-strain contribution (with the rate-of-strain evaluated at the sphere center), which is of the same form as when the sphere is in a linear field, plus a correction proportional to the Laplacian of the rate-of-strain (a third derivative of the velocity field).$\Diamond$

3.5.1 Ellipsoids and Spheroids

From the singularity solutions and multipole expansions for the ellipsoid, we obtain two forms of the Faxén laws for the ellipsoid:

$$\begin{aligned}
\boldsymbol{F} &= \mu\boldsymbol{A} \cdot \int_E f_{(1)}(\boldsymbol{x}')\{1 + \frac{c^2q^2\nabla^2}{2}\}\boldsymbol{v}^\infty(\boldsymbol{x}')dA(\boldsymbol{x}') - \mu\boldsymbol{A} \cdot \boldsymbol{U} \\
&= \mu\boldsymbol{A} \cdot \left(\frac{\sinh D}{D}\right)\boldsymbol{v}^\infty(\boldsymbol{x})|_{x=0} - \mu\boldsymbol{A} \cdot \boldsymbol{U}
\end{aligned}$$

$$\begin{aligned}
\boldsymbol{T} &= \mu\boldsymbol{C} \cdot \int_E f_{(2)}(\boldsymbol{x}')\{\frac{1}{2}\nabla \times \boldsymbol{v}^\infty - \boldsymbol{\omega}\}dA(\boldsymbol{x}') \\
&\quad + \mu\widetilde{\boldsymbol{H}} : \int_E f_{(2)}(\boldsymbol{x}')\{1 + \frac{c^2q^2\nabla^2}{6}\}e^\infty(\boldsymbol{x}')dA(\boldsymbol{x}') \\
&= \mu\boldsymbol{C} \cdot \left(\frac{3}{D}\frac{\partial}{\partial D}\right)\left(\frac{\sinh D}{D}\right)\frac{1}{2}\nabla \times \boldsymbol{v}^\infty(\boldsymbol{x})|_{x=0} - \mu\boldsymbol{C} \cdot \boldsymbol{\omega} \\
&\quad + \mu\widetilde{\boldsymbol{H}} : \left(\frac{3}{D}\frac{\partial}{\partial D}\right)\left(\frac{\sinh D}{D}\right)e^\infty(\boldsymbol{x})|_{x=0}
\end{aligned}$$

$$\begin{aligned}
\boldsymbol{S} &= \mu\boldsymbol{M} : \int_E f_{(2)}(\boldsymbol{x}')\{1 + \frac{c^2q^2\nabla^2}{6}\}e^\infty(\boldsymbol{x}')dA(\boldsymbol{x}') \\
&\quad + \mu\boldsymbol{H} \cdot \int_E f_{(2)}(\boldsymbol{x}')\{\frac{1}{2}\nabla \times \boldsymbol{v}^\infty - \boldsymbol{\omega}\}dA(\boldsymbol{x}') \\
&= \mu\boldsymbol{M} : \left(\frac{3}{D}\frac{\partial}{\partial D}\right)\left(\frac{\sinh D}{D}\right)e^\infty(\boldsymbol{x})|_{x=0} \\
&\quad + \mu\boldsymbol{H} \cdot \left(\frac{3}{D}\frac{\partial}{\partial D}\right)\left(\frac{\sinh D}{D}\right)\frac{1}{2}\nabla \times \boldsymbol{v}^\infty(\boldsymbol{x})|_{x=0} - \mu\boldsymbol{H} \cdot \boldsymbol{\omega} \ .
\end{aligned}$$

The symbolic operator (power series in D^2) form is efficient if the higher order terms in $(D^2)^k$ vanish rapidly with increasing k. However, the symbolic operator sum will not always converge. For example, consider the ambient field generated by the disturbance produced by a small particle translating near the ellipsoid. The series in $(D^2)^k\boldsymbol{v}^\infty = (D^2)^k\boldsymbol{F} \cdot \mathcal{G}(\boldsymbol{x} - \boldsymbol{y})/8\pi\mu$ will diverge if $\boldsymbol{y}$ is closer than a critical distance, as shown in Chapter 13. The integral form of the Faxén law

is always well defined for all $\boldsymbol{y}$ outside the ellipsoid and thus is the analytical continuation of the series.

The Faxén laws for the spheroid may be obtained by reduction of the results for the ellipsoid or by starting with the singularity solutions and applying the reciprocal theorem. The results for *prolate* spheroids are the most interesting, since the focal disk becomes the line segment between the two foci at $\pm k$ on the axis of symmetry, with $k = ae$. Consequently, the Faxén laws may be written in terms of line integrals of the ambient velocity field and its derivatives [50]:

$$\begin{aligned}
F_i &= 6\pi\mu a \left[X^A d_i d_j + Y^A(\delta_{ij} - d_i d_j)\right] \\
&\quad \times \frac{1}{2k}\int_{-k}^{k}\left\{1 + (k^2-\xi^2)\frac{(1-e^2)}{4e^2}\nabla^2\right\}(v_j^\infty - U_j)\,d\xi \\
T_i &= 8\pi\mu a^3\left[X^C d_i d_j + Y^C(\delta_{ij} - d_i d_j)\right] \\
&\quad \times \frac{3}{8k^3}\int_{-k}^{k}(k^2-\xi^2)((\nabla\times\boldsymbol{v}^\infty)_j - 2\omega_j)\,d\xi \\
&\quad - 8\pi\mu a^3 Y^H \epsilon_{ijl} d_l d_k \\
&\quad \times \frac{3}{4k^3}\int_{-k}^{k}\left\{(k^2-\xi^2)(1 + (k^2-\xi^2)\frac{(1-e^2)}{8e^2}\nabla^2\right\} e_{jk}^\infty\,d\xi \\
S_{ij} &= \frac{20}{3}\pi\mu a^3\left[X^M d_{ijkl}^{(0)} + Y^M d_{ijkl}^{(1)} + Z^M d_{ijkl}^{(2)}\right] \\
&\quad \times \frac{3}{4k^3}\int_{-k}^{k}\left\{(k^2-\xi^2)(1 + (k^2-\xi^2)\frac{(1-e^2)}{8e^2}\nabla^2\right\} e_{kl}^\infty\,d\xi \\
&\quad + \frac{20}{3}\pi\mu a^3\frac{3}{5}Y^H(\epsilon_{ikl}d_j + \epsilon_{jkl}d_i)d_l \\
&\quad \times \frac{3}{8k^3}\int_{-k}^{k}(k^2-\xi^2)((\nabla\times\boldsymbol{v}^\infty)_k - 2\omega_k)\,d\xi\ .
\end{aligned}$$

For a force-free and torque-free spheroid, we set $\boldsymbol{F} = \boldsymbol{T} = \boldsymbol{0}$ and obtain the following expressions for the translational and angular velocities:

$$\boldsymbol{U} = \frac{1}{2k}\int_{-k}^{k}\left\{1 + (k^2-\xi^2)\frac{(1-e^2)}{4e^2}\nabla^2\right\}\boldsymbol{v}^\infty\,d\xi$$

$$\begin{aligned}
\boldsymbol{\omega} &= \frac{3}{8k^3}\int_{-k}^{k}(k^2-\xi^2)\nabla\times\boldsymbol{v}^\infty\,d\xi \\
&+ \frac{e^2}{2-e^2}\frac{3}{4k^3}\int_{-k}^{k}\left\{(k^2-\xi^2)(1 + (k^2-\xi^2)\frac{(1-e^2)}{8e^2}\nabla^2\right\}\boldsymbol{d}\times(\boldsymbol{e}^\infty\cdot\boldsymbol{d})\,d\xi\ .
\end{aligned}$$

The orientation of the spheroid changes with time as

$$\begin{aligned}
\dot{\boldsymbol{d}} = \boldsymbol{\omega}\times\boldsymbol{d} &= \frac{3}{8k^3}\int_{-k}^{k}(k^2-\xi^2)(\nabla\times\boldsymbol{v}^\infty)\times\boldsymbol{d}\,d\xi \\
&+ \frac{e^2}{2-e^2}\frac{3}{4k^3}\int_{-k}^{k}\left\{(k^2-\xi^2)(1 + (k^2-\xi^2)\frac{(1-e^2)}{8e^2}\nabla^2\right\} \\
&\times (\boldsymbol{e}^\infty\cdot\boldsymbol{d} - \boldsymbol{e}^\infty : \boldsymbol{ddd})\,d\xi\ .
\end{aligned}$$

3.5.2 The Spherical Drop

The Faxén laws for viscous drops are also of the same functional form as the singularity solutions for the drop. The proof requires some extensions of the steps used for the rigid particle. We start with the reciprocal theorem and for $\boldsymbol{v}_1$ use the velocity field produced by a translating drop, while $\boldsymbol{v}_2$ is taken to be the field of a *stationary* drop near a point force at $\boldsymbol{y}$. The proof proceeds along identical lines to the one used for the rigid particle, up to the point where the boundary conditions are inserted into the reciprocal relation. We must have

$$\oint_S \boldsymbol{v}_1 \cdot (\boldsymbol{\sigma}_2 \cdot \boldsymbol{n})\, dS + \boldsymbol{v}_1(\boldsymbol{y}) \cdot \boldsymbol{F} = \oint_S \boldsymbol{v}_2 \cdot (\boldsymbol{\sigma}_1 \cdot \boldsymbol{n})\, dS \ . \tag{3.30}$$

At this point, it proves convenient to extract $\boldsymbol{U}$ from $\boldsymbol{v}_1$ so that the preceding equation becomes

$$\boldsymbol{U} \cdot \boldsymbol{F}_2 + \boldsymbol{v}_1(\boldsymbol{y}) \cdot \boldsymbol{F} = -\oint_S (\boldsymbol{v}_1 - \boldsymbol{U}) \cdot (\boldsymbol{\sigma}_2 \cdot \boldsymbol{n})\, dS + \oint_S \boldsymbol{v}_2 \cdot (\boldsymbol{\sigma}_1 \cdot \boldsymbol{n})\, dS \ . \tag{3.31}$$

The boundary conditions at the surface of the drop require that $\boldsymbol{n} \cdot \boldsymbol{v}_2 = 0$ and $\boldsymbol{n} \cdot (\boldsymbol{v}_1 - \boldsymbol{U}) = 0$, so only the *tangential* components of the surface traction are retained in the dot products. An application of the reciprocal theorem to the inner fields associated with $\boldsymbol{v}_1 - \boldsymbol{U}$ and $\boldsymbol{v}_2$ yields the relation,

$$\oint_S (\boldsymbol{v}_1^{(i)} - \boldsymbol{U}) \cdot (\boldsymbol{\sigma}_2^{(i)} \cdot \boldsymbol{n})\, dS = \oint_S \boldsymbol{v}_2^{(i)} \cdot (\boldsymbol{\sigma}_1^{(i)} \cdot \boldsymbol{n})\, dS \ . \tag{3.32}$$

Here again, it is understood that only the tangential component of the surface traction is retained. But in both problem 1 and 2, the tangential component of the traction is continuous across the interface. The preceding equation then implies that the two surface integrals in Equation 3.31 cancel. Again, we suppose that $\boldsymbol{v}_1$, the field produced by the translating drop, is available as a singularity solution, so that

$$\boldsymbol{v}_1(\boldsymbol{x}) = \boldsymbol{U} \cdot \mathcal{F}\{\mathcal{G}(\boldsymbol{x} - \boldsymbol{\xi})/8\pi\mu\} \ ,$$

where $\mathcal{F}$ is a linear functional and $\boldsymbol{\xi}$ represents the region over which the singularities are distributed. Using the same arguments as before, Equation 3.31 becomes

$$\boldsymbol{F}_2 = \mathcal{F}\{\boldsymbol{v}^{\infty}(\boldsymbol{\xi})\} \ ,$$

and we conclude that the Faxén law is of the same functional form as the singularity solution. For a spherical drop, we know the singularity solution and the Faxén law for the force follows immediately as

$$\boldsymbol{F} = 2\pi\mu_o a \left(\frac{2+3\lambda}{1+\lambda}\right) \left\{1 + \frac{\lambda a^2 \nabla^2}{2(2+3\lambda)}\right\} \boldsymbol{v}^{\infty}(\boldsymbol{x})|_{x=0} - 2\pi\mu_o a \left(\frac{2+3\lambda}{1+\lambda}\right) \boldsymbol{U} \ .$$

This was first shown by Hetsroni and Haber [38], who followed Faxén's approach.

The Faxén law for the stresslet on a spherical drop was first derived by Rallison [69]. For the sake of consistency we employ the standard proof, but Rallison's original proof contains essentially the same ideas.

In the reciprocal theorem, use for $\boldsymbol{v}_1$ the disturbance field of a drop in a rate-of-strain field, $\boldsymbol{E}\cdot\boldsymbol{x}$, and for $\boldsymbol{v}_2$, use the field of a *stationary* drop near a point force at $\boldsymbol{y}$. Because of the boundary condition $\boldsymbol{v}_1 = -\boldsymbol{E}\cdot\boldsymbol{x}$ on S_p, we obtain

$$\begin{aligned} -\boldsymbol{E} : \frac{1}{2}\oint_{S_p} (\boldsymbol{x}(\boldsymbol{\sigma}\cdot\boldsymbol{n}) + \boldsymbol{x}(\boldsymbol{\sigma}\cdot\boldsymbol{n}))\, dS + \boldsymbol{v}_1(\boldsymbol{y})\cdot\boldsymbol{F} \\ = -\oint_{S_p} (\boldsymbol{v}_1 + \boldsymbol{E}\cdot\boldsymbol{x})\cdot(\boldsymbol{\sigma}_2\cdot\boldsymbol{n})\, dS + \oint_{S_p} \boldsymbol{v}_2\cdot(\boldsymbol{\sigma}_1\cdot\boldsymbol{n})\, dS\ . \end{aligned} \tag{3.33}$$

The boundary conditions at the surface of the drop require that $\boldsymbol{n}\cdot\boldsymbol{v}_2 = 0$ and $\boldsymbol{n}\cdot(\boldsymbol{v}_1 + \boldsymbol{E}\cdot\boldsymbol{x}) = 0$, so again, only the *tangential* components of the surface traction are retained in the dot products. An application of the reciprocal theorem to the inner fields associated with $\boldsymbol{v}_1 - \boldsymbol{U}$ and $\boldsymbol{v}_2$ yields the relation,

$$\oint_S (\boldsymbol{v}_1^{(i)} + \boldsymbol{E}\cdot\boldsymbol{x})\cdot(\boldsymbol{\sigma}_2^{(i)}\cdot\boldsymbol{n})\, dS = \oint_S \boldsymbol{v}_2^{(i)}\cdot(\boldsymbol{\sigma}_1^{(i)}\cdot\boldsymbol{n} + 2\mu_i\boldsymbol{E}\cdot\boldsymbol{n})\, dS\ ,$$

where again it is understood that only the tangential components of the surface tractions are retained. Again, the tangential components of the traction are continuous across the interface, so that the preceding equation becomes

$$\oint_S (\boldsymbol{v}_1 + \boldsymbol{E}\cdot\boldsymbol{x})\cdot(\boldsymbol{\sigma}_2\cdot\boldsymbol{n})\, dS = \oint_S \boldsymbol{v}_2\cdot(\boldsymbol{\sigma}_1\cdot\boldsymbol{n} + 2\mu_o\boldsymbol{E}\cdot\boldsymbol{n})\, dS\ ,$$

and Equation 3.33 simplifies to

$$\boldsymbol{E} : \left[\frac{1}{2}\oint_S (\boldsymbol{x}(\boldsymbol{\sigma}_2\cdot\boldsymbol{n}) + \boldsymbol{x}(\boldsymbol{\sigma}_2\cdot\boldsymbol{n}))\, dS - \mu_o\oint_S (\boldsymbol{v}_2\boldsymbol{n} + \boldsymbol{n}\boldsymbol{v}_2)\, dS\right] = \boldsymbol{v}_1(\boldsymbol{y})\cdot\boldsymbol{F}\ .$$

We recognize the quantity inside the brackets on the left hand side of this equation as the stresslet, $\boldsymbol{S}_2$.

Again, suppose that $\boldsymbol{v}_1$, the disturbance field of the drop in a rate-of-strain field is in the form of a singularity solution,

$$\boldsymbol{v}_1(\boldsymbol{x}) = \boldsymbol{E} : \mathcal{S}\{\mathcal{G}(\boldsymbol{x}-\boldsymbol{\xi})/8\pi\mu\}\ ,$$

where $\mathcal{S}$ is a linear functional and $\boldsymbol{\xi}$ represents the region over which the singularities are distributed. Using the same arguments as before, we conclude that

$$\boldsymbol{S}_2 = \mathcal{F}\{\boldsymbol{v}^\infty(\boldsymbol{\xi})\}\ .$$

This singularity solution is derived for a spherical drop in Exercise 3.7, and based on that result, the Faxén law for the stresslet follows as

$$\boldsymbol{S} = \frac{4}{3}\pi\mu_o a\left(\frac{2+5\lambda}{1+\lambda}\right)\left\{1 + \frac{\lambda a^2\nabla^2}{2(2+5\lambda)}\right\} e^\infty(\boldsymbol{x})|_{x=0}\ .$$

Exercises

Exercise 3.1 The Integral Representation for the Disturbance Field of a Viscous Drop.
Derive the integral representation for the disturbance field of a viscous drop:

$$\begin{aligned} \boldsymbol{v}(\boldsymbol{x}) - \boldsymbol{v}^{\infty}(\boldsymbol{x}) &= -\frac{1}{8\pi\mu}\oint_S (\boldsymbol{\sigma}(\boldsymbol{\xi})\cdot\hat{\boldsymbol{n}})\cdot\mathcal{G}(\boldsymbol{x}-\boldsymbol{\xi})\, dS(\boldsymbol{\xi}) \\ &\quad - \oint_S \boldsymbol{v}(\boldsymbol{\xi})\cdot(\boldsymbol{\Sigma}\cdot\hat{\boldsymbol{n}})\, dS(\boldsymbol{\xi}) \ . \end{aligned}$$

Use the analogous representation for the flow inside the drop to derive the following representation in terms of a traction jump across the interface and a double layer potential [68, 70]

$$\begin{aligned} \frac{1}{2}\boldsymbol{v}(\boldsymbol{\xi}) &= -\frac{1}{8\pi\mu}\frac{1}{1+\lambda}\oint_S ([\boldsymbol{\sigma}^{(o)} - \boldsymbol{\sigma}^{(i)}](\boldsymbol{\xi})\cdot\hat{\boldsymbol{n}})\cdot\mathcal{G}(\boldsymbol{x}-\boldsymbol{\xi})\, dS(\boldsymbol{\xi}) \\ &\quad - \left(\frac{1-\lambda}{1+\lambda}\right)\oint_S \boldsymbol{v}(\boldsymbol{\xi})\cdot(\boldsymbol{\Sigma}(\boldsymbol{x}-\boldsymbol{\xi})\cdot\hat{\boldsymbol{n}})\, dS(\boldsymbol{\xi}) \ . \end{aligned}$$

Exercise 3.2 The Stresslet for a Viscous Drop.
Expand the integral representation of the previous exercise and show that the stresslet on a viscous drop is given by

$$\boldsymbol{S} = \frac{1}{2}\oint_S [(\boldsymbol{\sigma}\cdot\hat{\boldsymbol{n}})\boldsymbol{\xi} + \boldsymbol{\xi}(\boldsymbol{\sigma}\cdot\hat{\boldsymbol{n}})]\, dS - \frac{1}{3}\oint_S (\boldsymbol{\sigma}\cdot\hat{\boldsymbol{n}})\cdot\boldsymbol{\xi}\ dS\ \boldsymbol{\delta} - \mu\oint_{S_p} (\boldsymbol{v}\hat{\boldsymbol{n}} + \hat{\boldsymbol{n}}\boldsymbol{v})\ dS \ .$$

Exercise 3.3 The Spheroidal Harmonics.
When the Laplace equation $\nabla^2\Phi = 0$ is separated in prolate spheroidal coordinates (η, θ, ϕ),

$$\begin{aligned} x &= c\sinh\eta\sin\theta\cos\phi \\ y &= c\sinh\eta\sin\theta\sin\phi \\ z &= c\cosh\eta\cos\theta \ , \end{aligned}$$

the solution may be written as [42]

$$\Phi(\eta,\theta,\phi) = P_n(\cosh\eta)P_n(\cos\theta)e^{im\phi} \ .$$

Find the relation between these solutions and G_n.

Exercise 3.4 Degenerate Limits for the Ellipsoid.
Show that the singularity solution and image system of the general triaxial ellipsoid reduce to that for the prolate spheroid in the limit of vanishing $b_E = \sqrt{b^2 - c^2}$.
Hint: In the limit of small b_E/a_E, replace $\mathcal{G}(\boldsymbol{x},\boldsymbol{\xi})$ with its Taylor series in ξ_2 about $\xi_2 = 0$; then show that the higher order terms vanish and that the leading term, after integration with respect to ξ_2, gives the singularity density of the prolate spheroid solution.

Exercise 3.5 Relation Between the Solutions for Prolate and Oblate Spheroids.
Show that the resistance functions for the prolate and oblate spheroids can be obtained from one another by switching the roles played by a and c, or equivalently, by replacing the eccentricity e everywhere by $ie/\sqrt{1-e^2}$, using the properties of the complex trigonometric and logarithmic functions.

Exercise 3.6 The Faxén Law for the Torque and Stresslet.
Relate the Faxén law for the torque and stresslet on a general particle and the particle's singularity solutions for rotation and rate-of-strain fields.

Exercise 3.7 The Singularity Solution for a Drop in a Rate-of-Strain Field.
Show that the singularity solution for a spherical drop in a rate of strain field is

$$\boldsymbol{v} = \boldsymbol{E}\cdot\boldsymbol{x} + 2\pi\mu_o a(\boldsymbol{E}\cdot\nabla)\cdot\left(\frac{2+5\lambda}{1+\lambda}\right)\left\{1+\frac{\lambda a^2\nabla^2}{2(2+5\lambda)}\right\}\frac{\mathcal{G}(\boldsymbol{x})}{8\pi\mu}\,.$$

Note that as $\lambda\to\infty$, we recover the solution for the rigid sphere, while $\lambda = 0$ (bubble) requires just the stresslet field. The singularity solution pertains to the exterior flow field. Inside the drop, the velocity should be represented as a linear combination to $\boldsymbol{E}\cdot\boldsymbol{x}$ and a cubic field.

In this solution for the viscous drop, the normal forces *are not* balanced. When surface tension forces dominate over viscous forces, the shape of the surface may be determined in an iterative fashion, with the above solution providing the leading term [22]. For the general case, a numerical approach is required, *e.g.*, [70].